Large Scale dynamics of Brown trout populations across Navarra' Rivers (North Spain)

Alonso, C., García de Jalón, D., Álvarez, J. , Gortázar, J.

Advances in the Population Ecology of Stream Salmonids

ecohidráulica

Grupo Investigación HIDROBIOLOGÍA
UNIVERSIDAD POLITÉCNICA DE MADRID

GESTION AMBIENTAL
VIVEROS Y REPOBLACIONES
DE NAVARRA S.A.

Introduction

Relevance of population ecology

To determine to what extent exogenous and endogenous factors drive the temporal variation of population abundance is a key issue of population ecology.

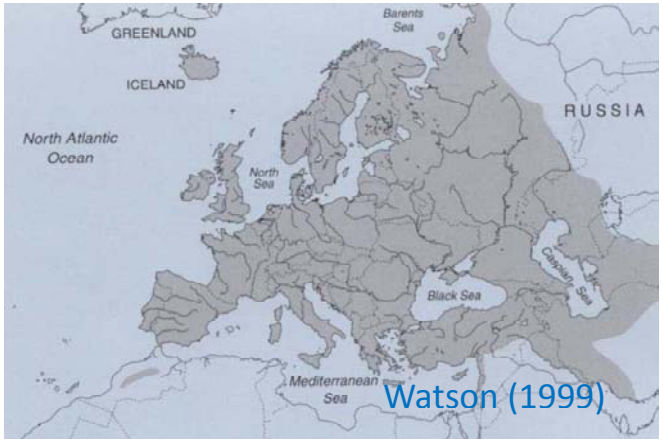

Watson (1999)

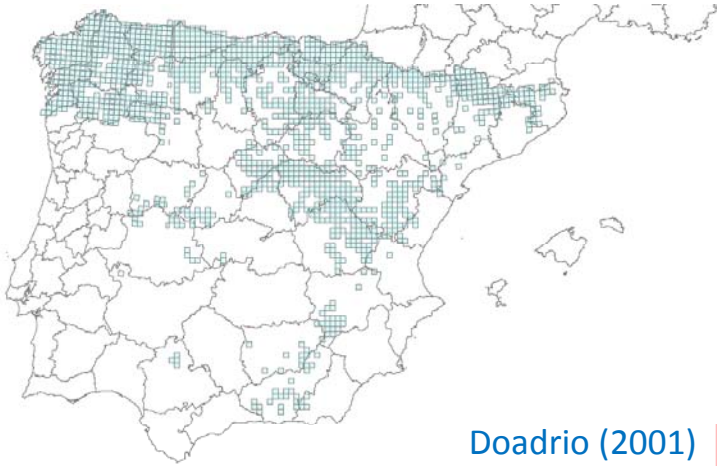

Doadrio (2001)

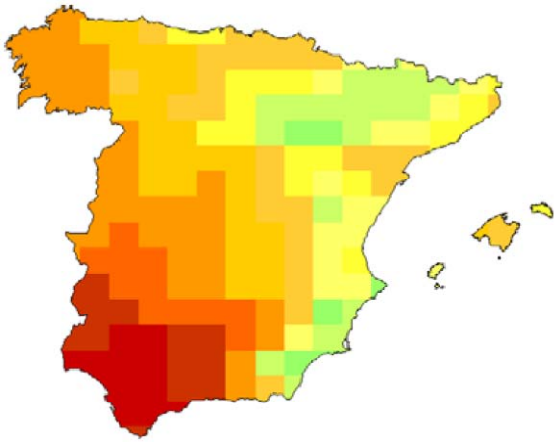

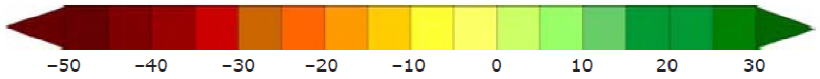

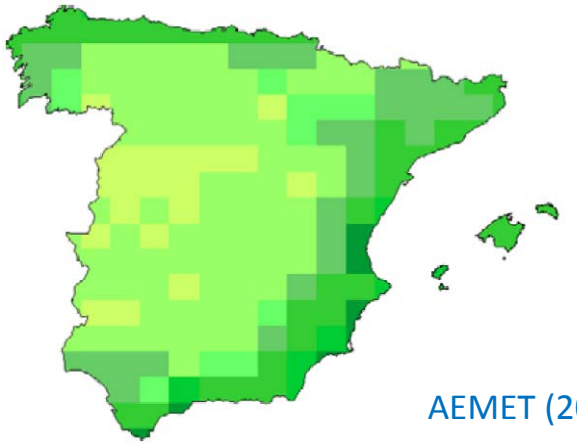

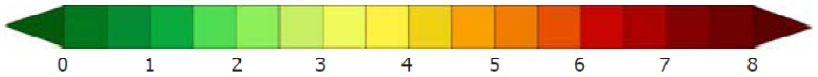

AEMET (2009)

Anual rainfall and **mean temperature**

estimated changes in for the period 2011-2040, compared to the control period (1961-1990).

Introduction

Context

-Time series of brown trout populations in Navarra (North Spain) showed a decreasing abundance for the last decade: recreational angling was prohibited in 2008.

-An exploratory approach was addressed.

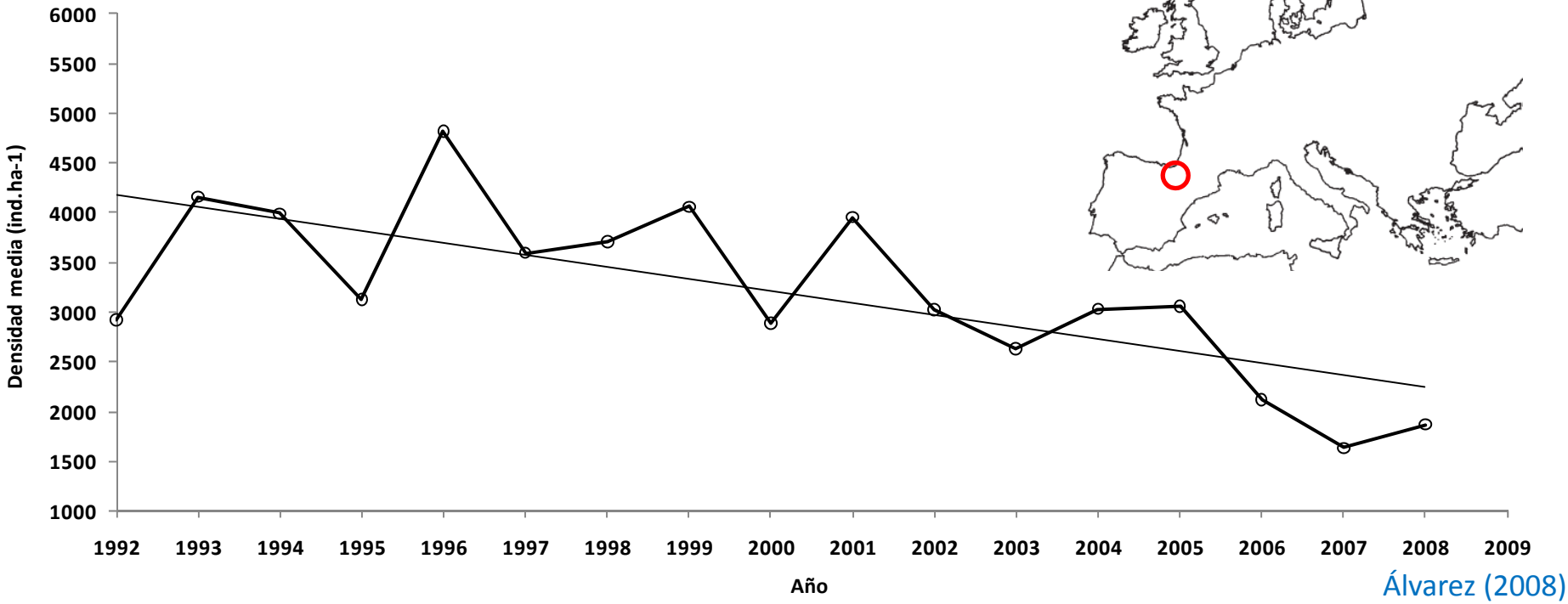

Álvarez (2008)

Mean density (n.ha-1) of brown trout in Navarra during the period 1992-2008.

Introduction

General scope

Most studies on the population dynamics of stream-living salmonids have attempted to elucidate the causes of variation in demographic traits or population abundance by analyzing population time series vs. environmental data.

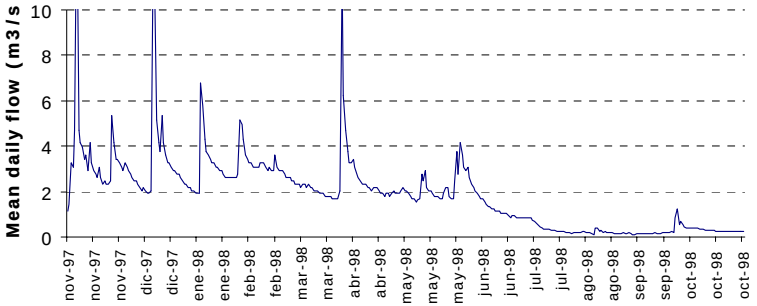

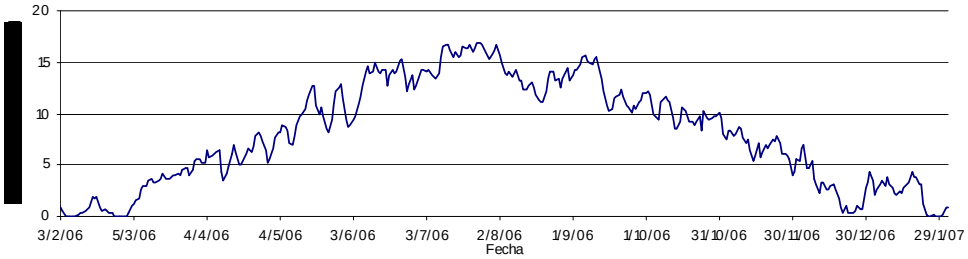

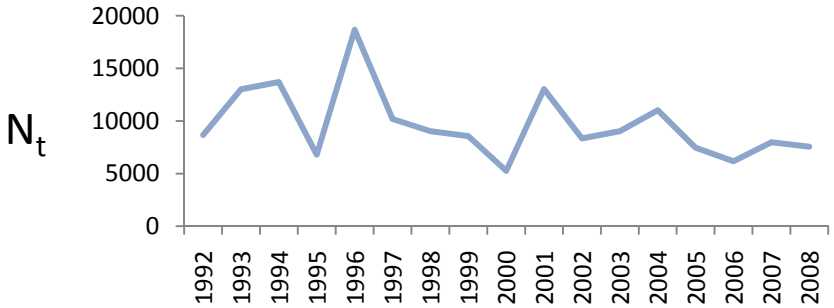

Introduction

General focus

In order to express the results on a scale compatible with fishery management strategies, most studies have been done at the scale of a stream reach, a stream or a river basin with few studies analyzing the variation of mean abundances at larger geographic scales.

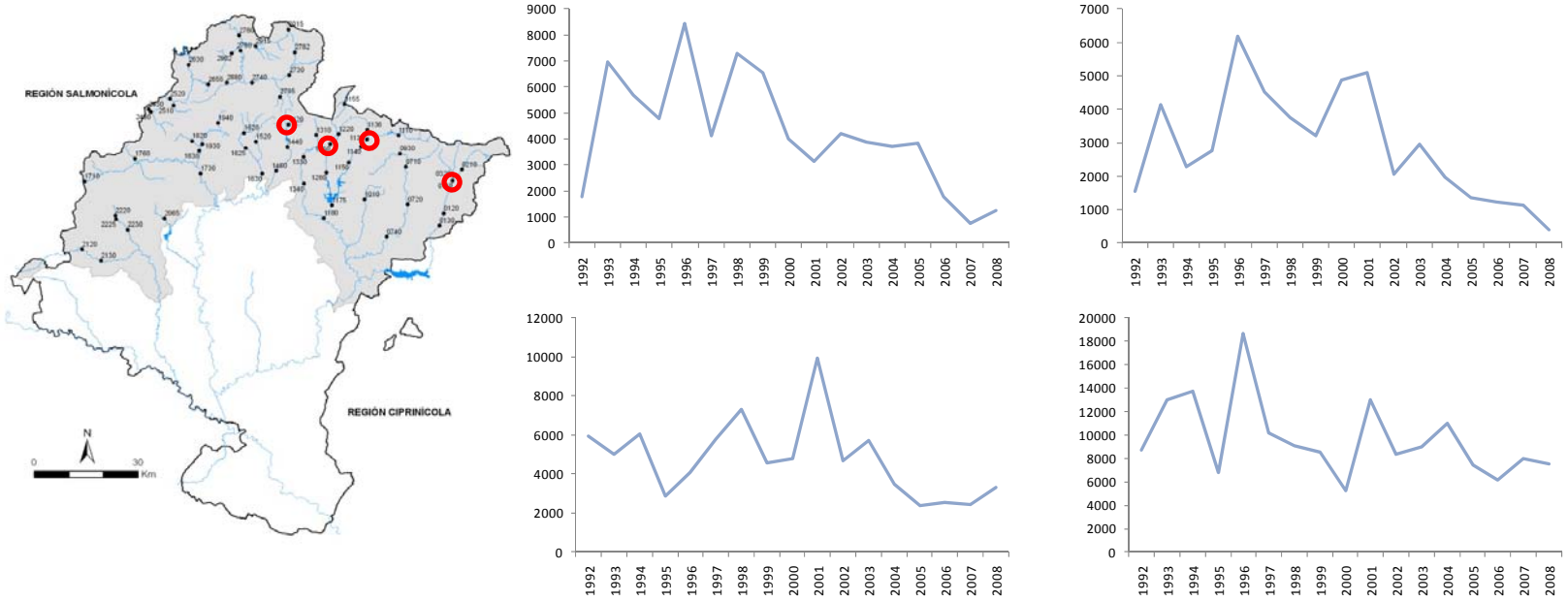

Introduction

General focus

The temporal variation of the size of a given population can be determined by variables that are relevant at the reach or basin scale. But if the variables driving separated independent populations are found , these are likely to be provide better knowledge on the autoecology of the species.

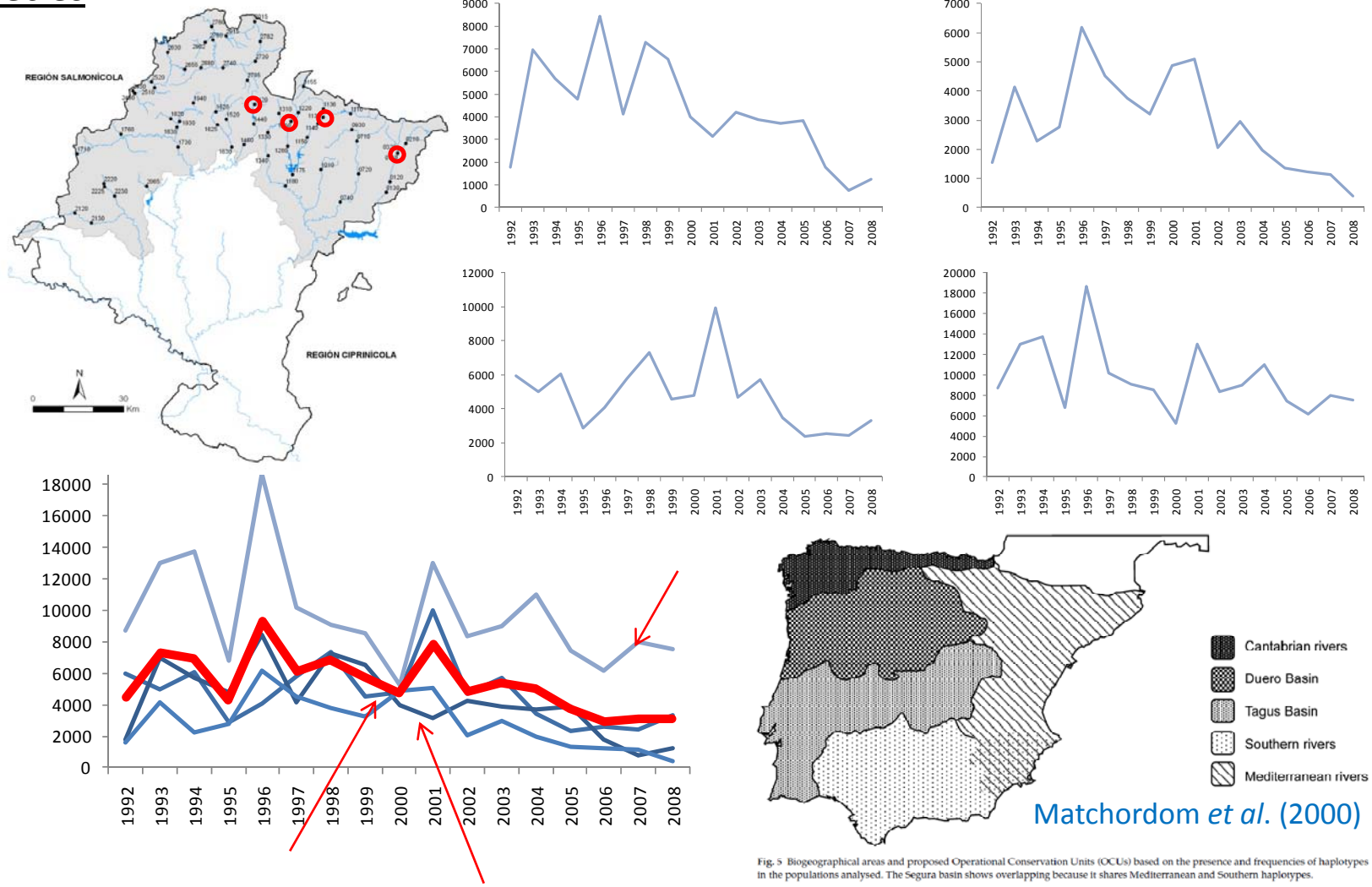

Fig. 5 Biogeographical areas and proposed Operational Conservation Units (OCUs) based on the presence and frequencies of haplotypes in the populations analysed. The Segura basin shows overlapping because it shares Mediterranean and Southern haplotypes.

Study area

An heterogeneous area

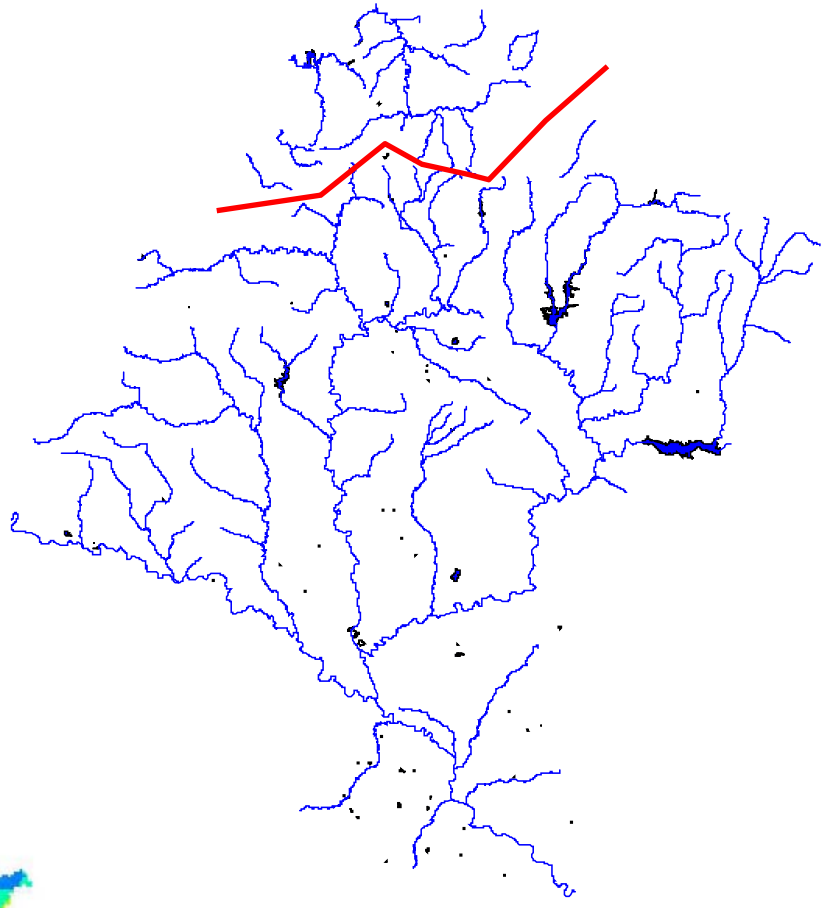

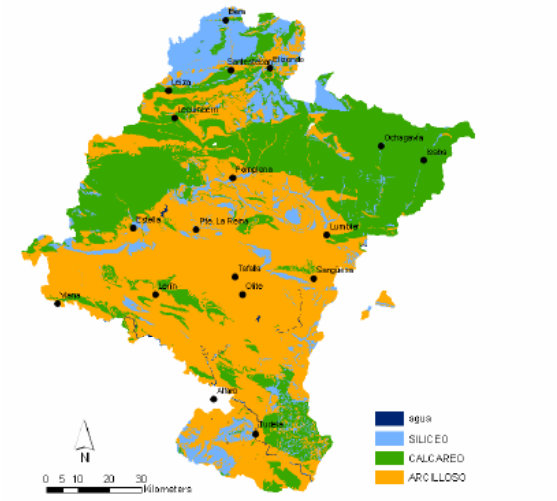

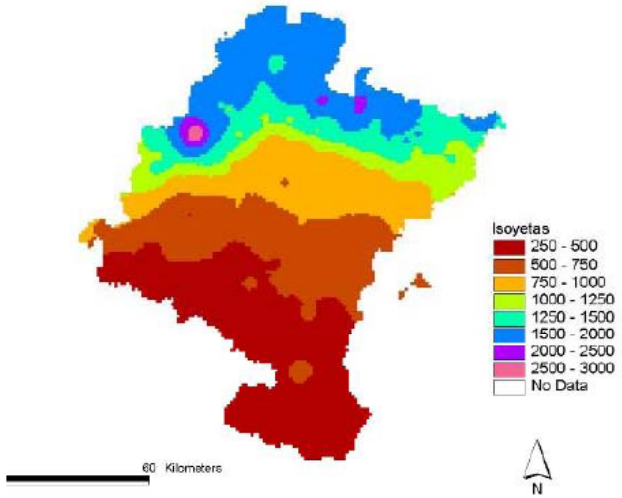

Methods

Endogenous variables: 0+ , 1+ and adult densities

n = 61 sampling sites
During 17 years

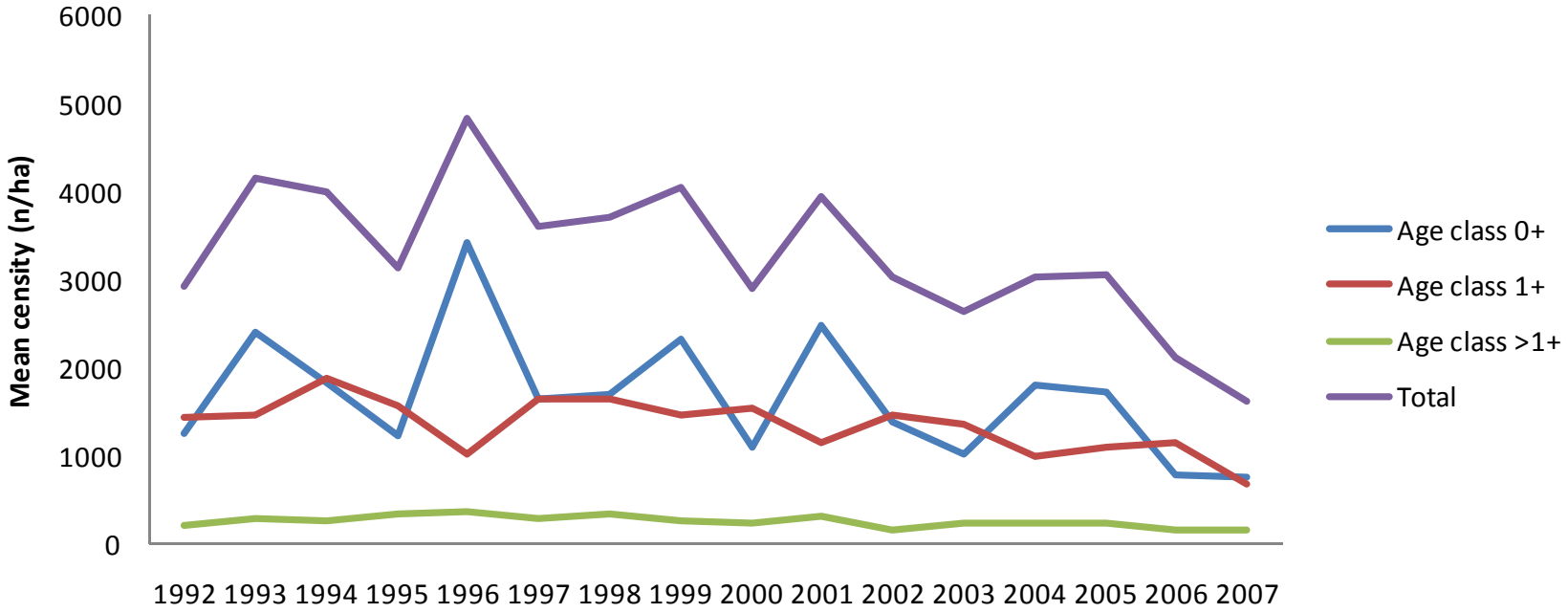

Methods

Exogenous driver: “process window”

The exogenous driver must fulfill what Stenseth & Mysterud (2005) call “the time window component, the spatial window component and the weather composition component” meaning temporal, spatial and climatic scales.

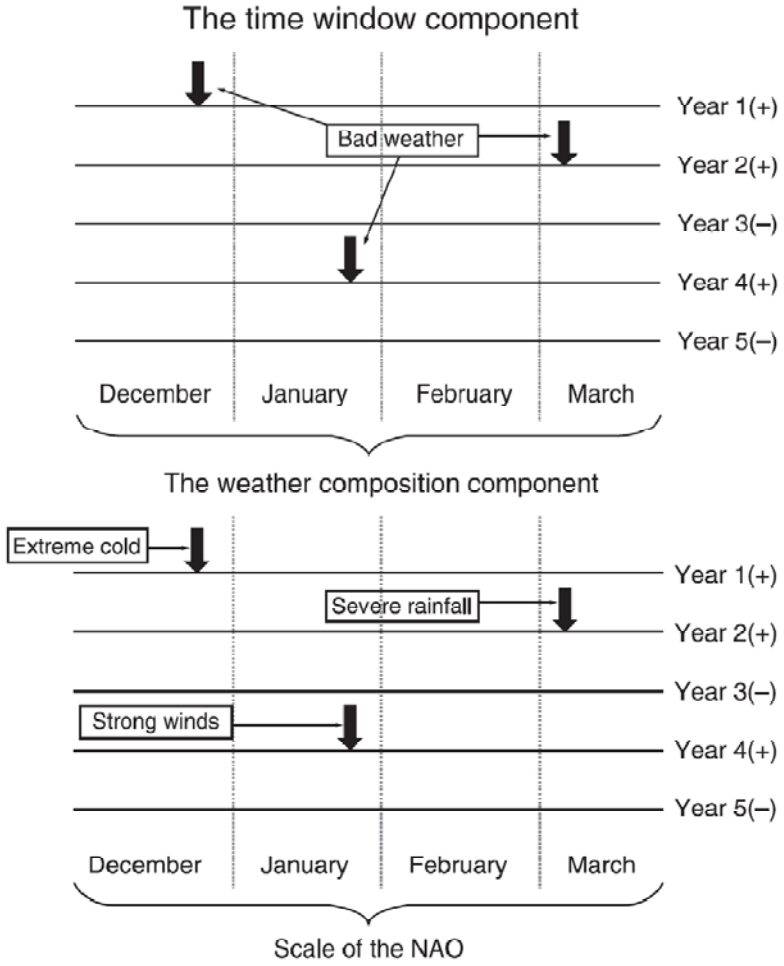

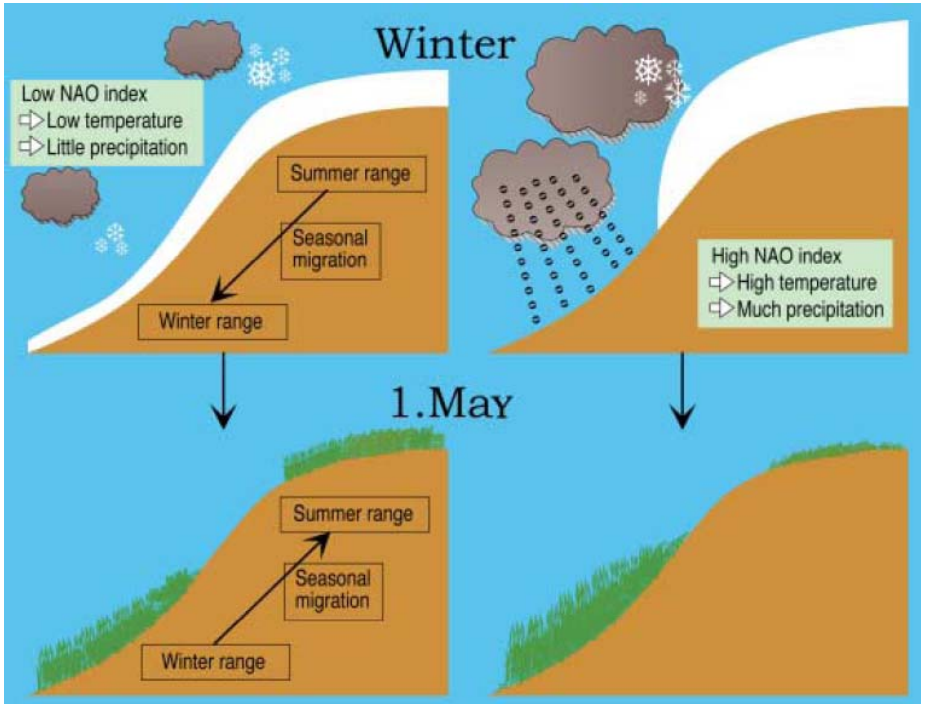

Stenseth & Mysterud (2005)

The time, spatial and weather window components of climate (Hallett *et al.* 2004) provides a mechanism for explaining why the NAO may better explain the dynamics of animal populations than monthly averages of local climate.

Methods

Exogenous driver: North Atlantic Oscillation

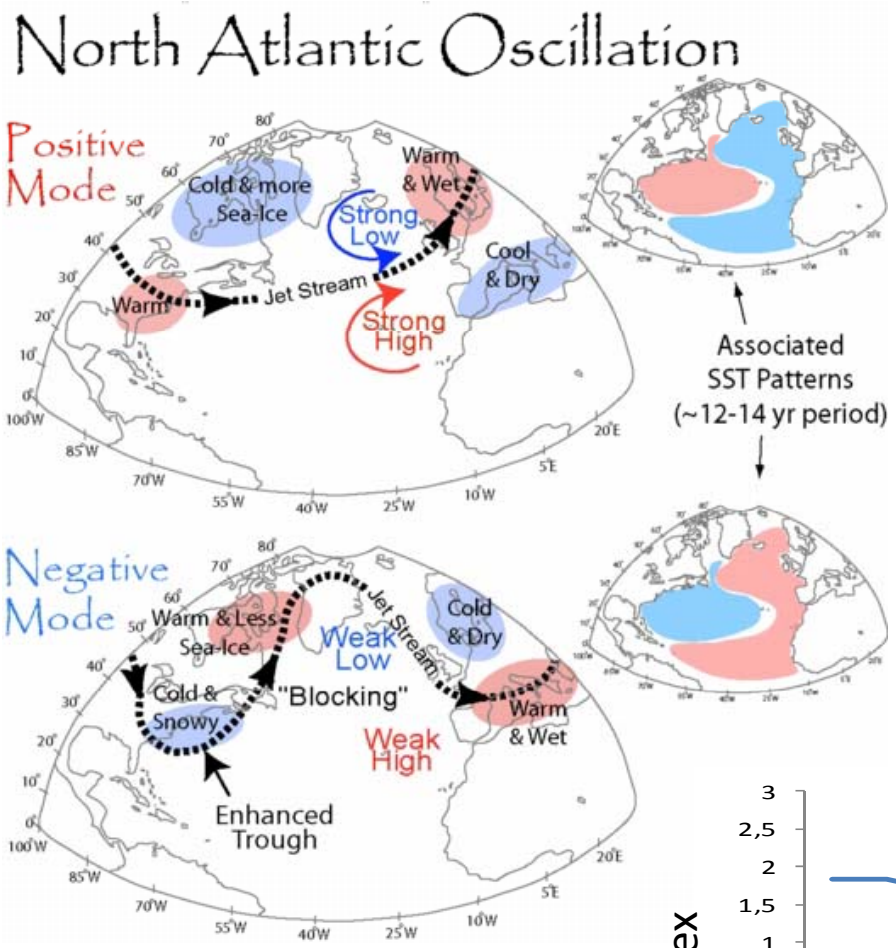

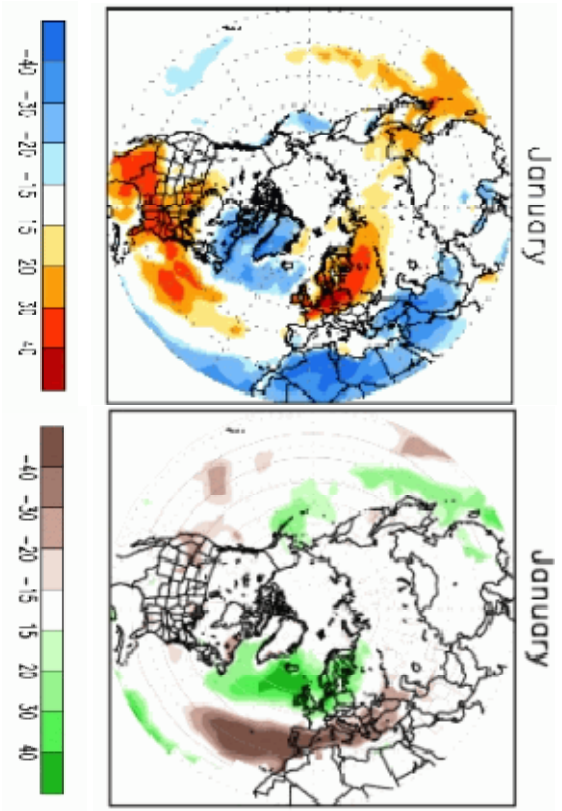

Temperature

Rainfall

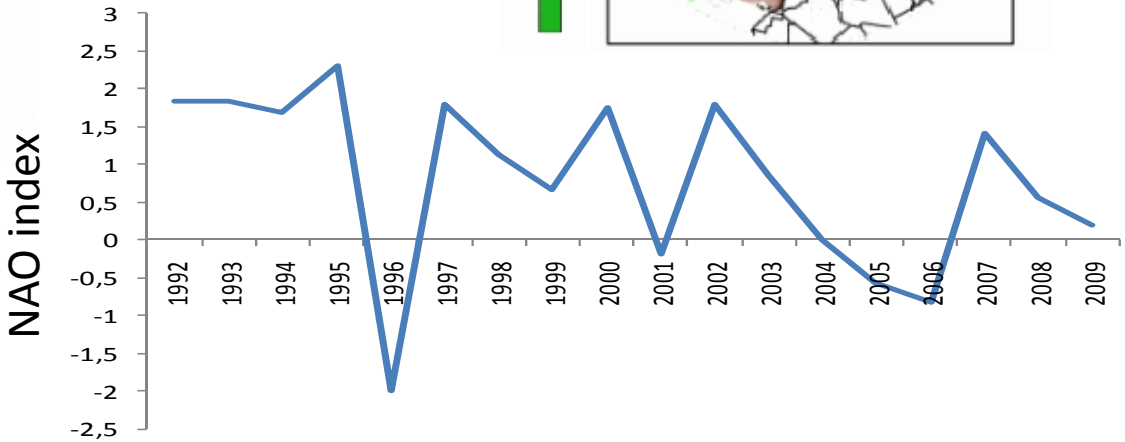

Methods

Population growth rate (*pgr*): non-structured model

The value of *pgr* is influenced by **endogenous (x_i)** and **exogenous (y_i)** factors and its variation can be expressed as a function of those variables (r function), taking into account **non-additivity**:

$$\lambda_t = f(x_{1,t}, x_{2,t} \ldots x_{n,t}, y_{1,t}, y_{2,t} \ldots y_{m,t}, x_{1,t} \times y_{1,t} \ldots x_{1,t} \times y_{m,t}, x_{2,t} \times y_{1,t} \ldots x_{2,t} \times y_{m,t} \ldots x_{n,t} \times y_{1,t} \ldots x_{n,t} \times y_{m,t})$$

$$\lambda_t = \frac{N_{t+1}}{N_t}$$

$$r_t = \log_e \lambda_t = \log_e \frac{N_{t+1}}{N_t}$$

Age-structured model

A demographic approach was made by conducting the same steps using each age class per capita growth rate: λ^{0+}_t, λ^{1+}_t and $\lambda^{\geq 2+}_t$ as dependent variable. Starting from the definition of population growth rate:

$$\lambda_t = N_{t+1}/N_t = (N^{0+}_{t+1}+N^{1+}_{t+1}+N^{\geq 2+}_{t+1})/N_t = (N^{0+}_{t+1}/N_t)+(N^{1+}_{t+1}/N_t)+(N^{\geq 2+}_{t+1}/N_t)$$
$$= \lambda^{0+}_t+\lambda^{1+}_t+\lambda^{\geq 2+}_t$$

therefore:

$$\lambda^{0+}_t=f(x_{1,t},x_{2,t},\dots x_{n,t},y_{1,t},y_{2,t},\dots y_{m,t},x_{1,t}\times y_{1,t},\dots x_{1,t}\times y_{m,t},x_{2,t}\times y_{1,t},\dots x_{2,t}\times y_{m,t},\dots x_{n,t}\times y_{1,t},\dots x_{n,t}\times y_{m,t})$$

$$\lambda^{1+}_t=f(x_{1,t},x_{2,t},\dots x_{n,t},y_{1,t},y_{2,t},\dots y_{m,t},x_{1,t}\times y_{1,t},\dots x_{1,t}\times y_{m,t},x_{2,t}\times y_{1,t},\dots x_{2,t}\times y_{m,t},\dots x_{n,t}\times y_{1,t},\dots x_{n,t}\times y_{m,t})$$

$$\lambda^{\geq 2+}_t=f(x_{1,t},x_{2,t},\dots x_{n,t},y_{1,t},y_{2,t},\dots y_{m,t},x_{1,t}\times y_{1,t},\dots x_{1,t}\times y_{m,t},x_{2,t}\times y_{1,t},\dots x_{2,t}\times y_{m,t},\dots x_{n,t}\times y_{1,t},\dots x_{n,t}\times y_{m,t})$$

Non-structured model

Estimates of the regression coefficients, their standard error and the P-value of the selected variables in the descriptive model of λ_t.

Parameter	Estimate	Standard error	P-value
Constant	1,485	0,304	0,002
$NAO_{w,t}$	-0,377	0,155	0,045
$NAO_{w,t+1}$	-0,832	0,233	0,009
N_t	-0,000484	0,000123	0,006
N_{t-2}	0,000263	4,72E-05	0,001
$N_{t-1} \times NAO_{w,t}$	0,000126	4,08E-05	0,018
$N_t \times NAO_{w,t+1}$	0,000234	7,27E-05	0,015

Non-structured model

Estimates of the regression coefficients, their standard error and the P-value of the selected variables in the descriptive model of λ_t.

Parameter	Estimate	Standard error	P-value
Constant	1,485	0,304	0,002
$NAO_{w,t}$	-0,377	0,155	0,045
$NAO_{w,t+1}$	-0,832	0,233	0,009
N_t	-0,000484	0,000123	0,006
N_{t-2}	0,000263	4,72E-05	0,001
$N_{t-1} \times NAO_{w,t}$	0,000126	4,08E-05	0,018
$N_t \times NAO_{w,t+1}$	0,000234	7,27E-05	0,015

Non-structured model

Estimates of the regression coefficients, their standard error and the P-value of the selected variables in the descriptive model of λ_t.

Parameter	Estimate	Standard error	P-value
Constant	1,485	0,304	0,002
$NAO_{w,t}$	-0,377	0,155	0,045
$NAO_{w,t+1}$	-0,832	0,233	0,009
N_t	-0,000484	0,000123	0,006
N_{t-2}	0,000263	4,72E-05	0,001
$N_{t-1} \times NAO_{w,t}$	0,000126	4,08E-05	0,018
$N_t \times NAO_{w,t+1}$	0,000234	7,27E-05	0,015

Non-structured model

Estimates of the regression coefficients, their standard error and the P-value of the selected variables in the descriptive model of λ_t.

Parameter	Estimate	Standard error	P-value
Constant	1,485	0,304	0,002
$NAO_{w,t}$	-0,377	0,155	0,045
$NAO_{w,t+1}$	-0,832	0,233	0,009
N_t	-0,000484	0,000123	0,006
N_{t-2}	0,000263	4,72E-05	0,001
$N_{t-1} \times NAO_{w,t}$	0,000126	4,08E-05	0,018
$N_t \times NAO_{w,t+1}$	0,000234	7,27E-05	0,015

Age-structured model

Estimates of the regression coefficients and the P-value of the selected variables in the descriptive model of $\lambda^{0+}{}_t$, $\lambda^{1+}{}_t$ and $\lambda^{\geq 2+}{}_t$.

Dependent variable	Parameter	Estimate	P-value	Adjusted r^2
$\lambda^{1}{}_t$	Constant	0,221	0,322	0,85
	N_t	-1,79E-04	0,041	
	N_{t-2}	2,57E-04	0,001	
	$N_t \times NAO_{w,t+1}$	9,61E-05	0,036	
	$N_{t-2} \times NAO_{w,t+1}$	-0,000121	0,007	
$\lambda 2_t$	Constant	0,360052	0	0,47
	$NAO_{w,t}$	0,022521	0,008	
	$N_{t-1} \times NAO_{w,t+1}$	4,41E-06	0,046	
$\lambda 3_t$	Constant	0,074123	0	0,68
	$N_t \times NAO_{w,t+1}$	-2,58E-06	0,007	
	$N_{t-1} \times NAO_{s,t+1}$	-2,66E-06	0,032	
	$N_{t-1} \times NAO_{w,t}$	2,49E-06	0,005	

Results

Model plot

Non-structured model

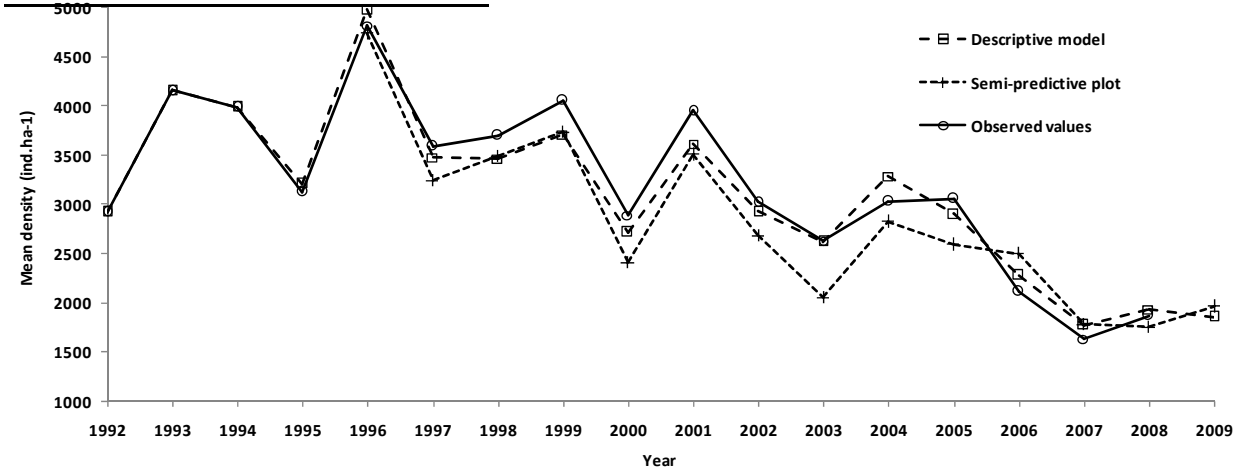

Age-structured model

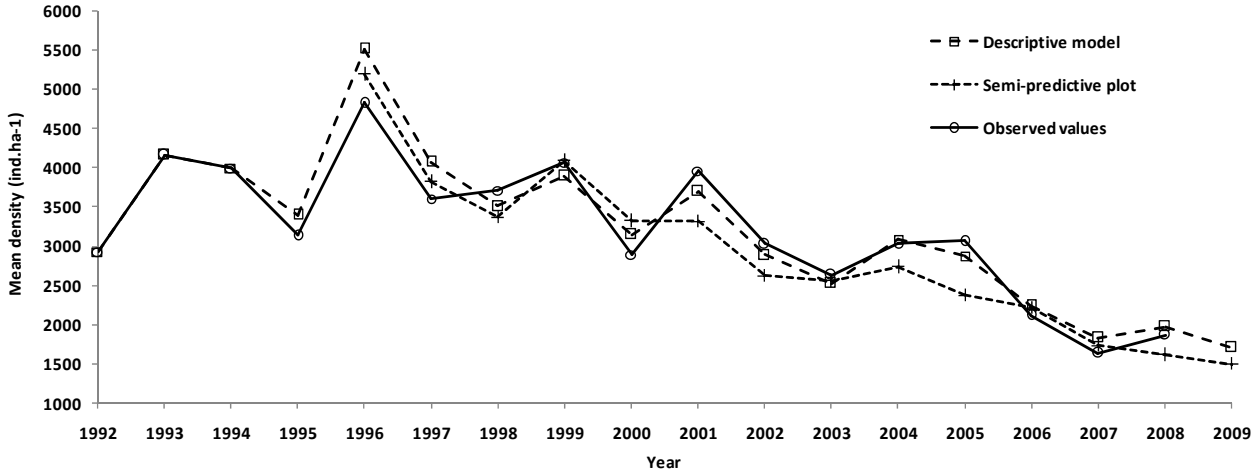

Results of the fitted non-structured (top) and age-structured (bottom) *descriptive and predictive plots* represented against time.

Results

Model plot

Non-structured model

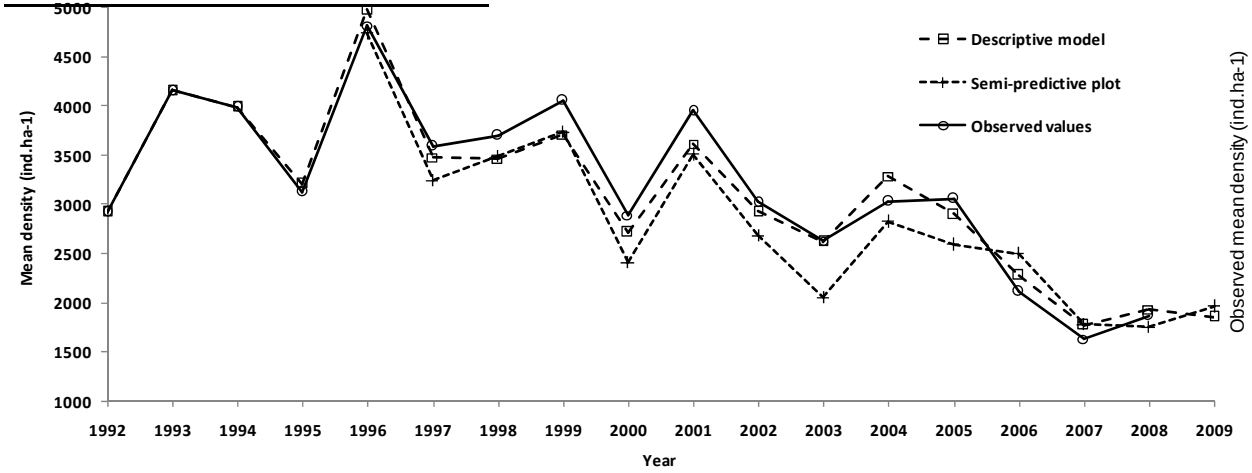

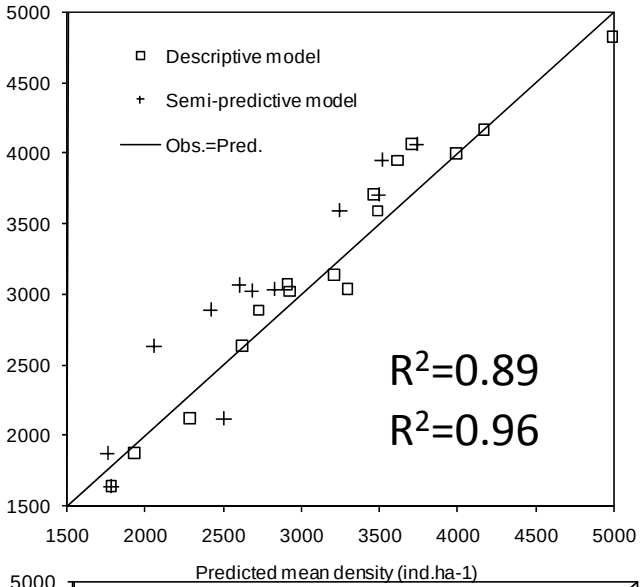

Age-structured model

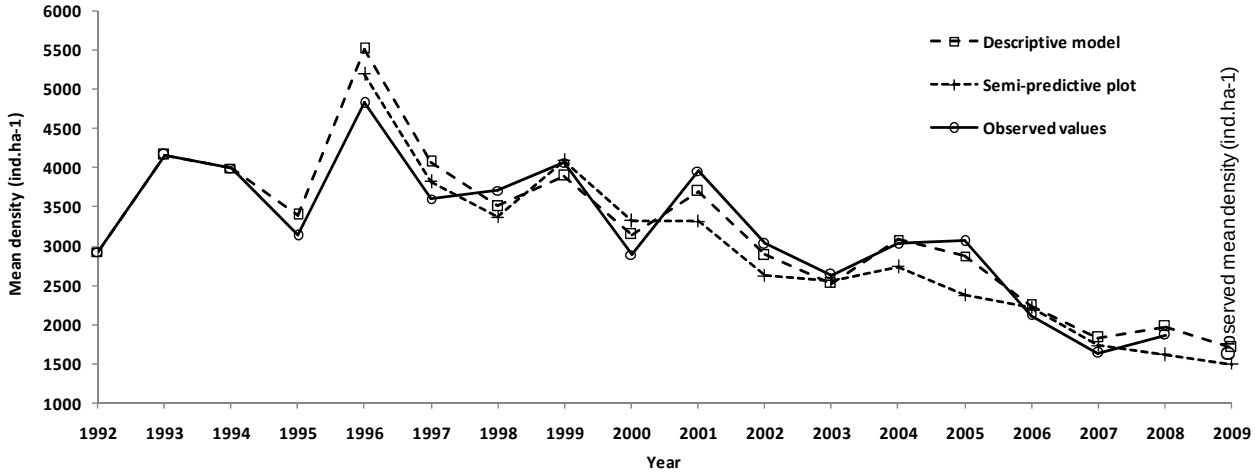

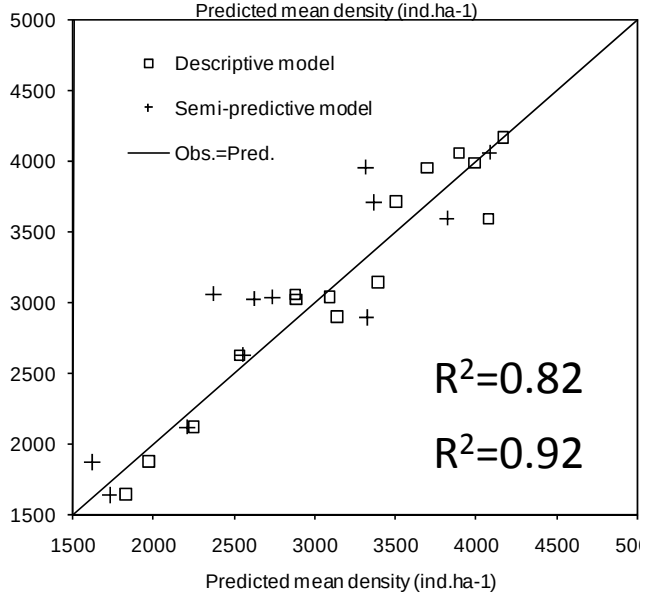

Results of the fitted non-structured (top) and age-structured (bottom) *descriptive and predictive plots* represented against time (left) and observed vs. modeled (right).

Results

Model predictions

Non-structured model

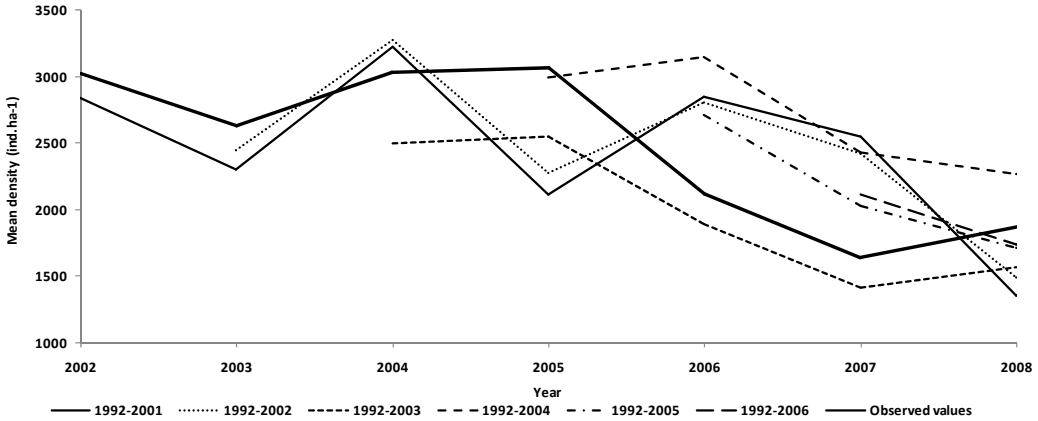

Age-structured model

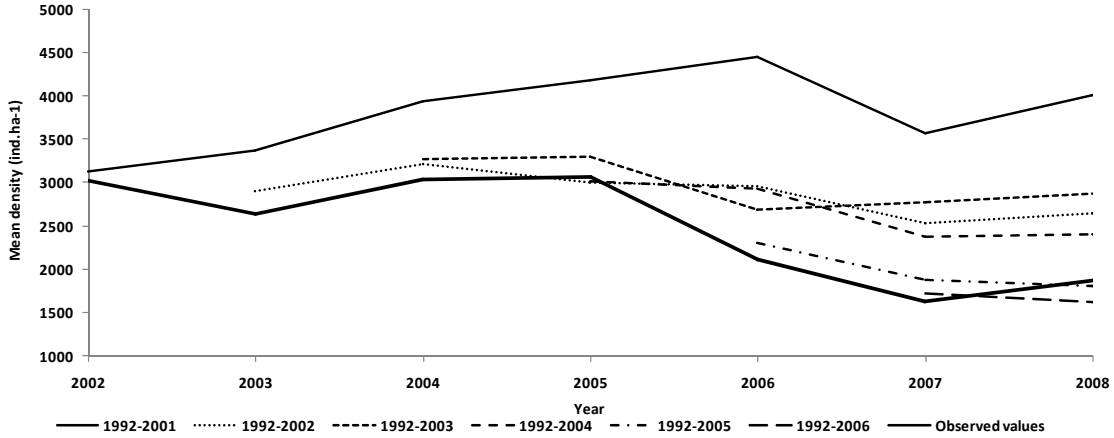

Estimated mean densities Nt obtained from iteration of non-structured (top) and age-structured (bottom) predictive model fitted to different data time series.

Results

Model predictions

Non-structured model

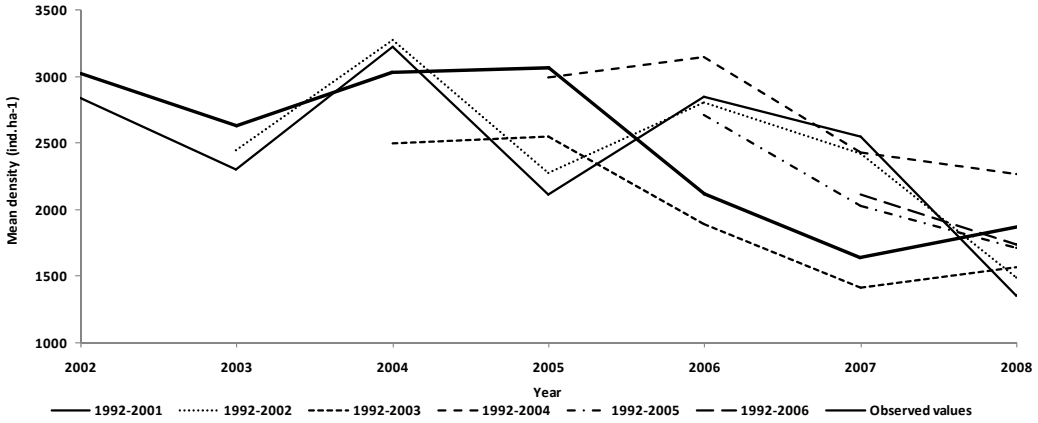

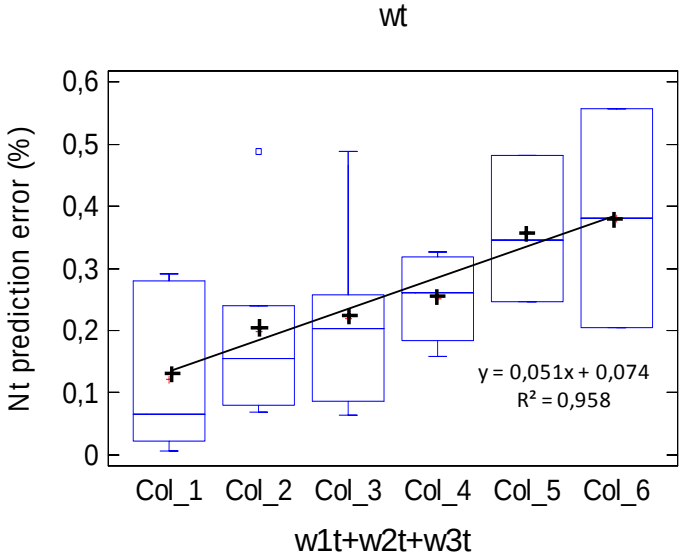

Age-structured model

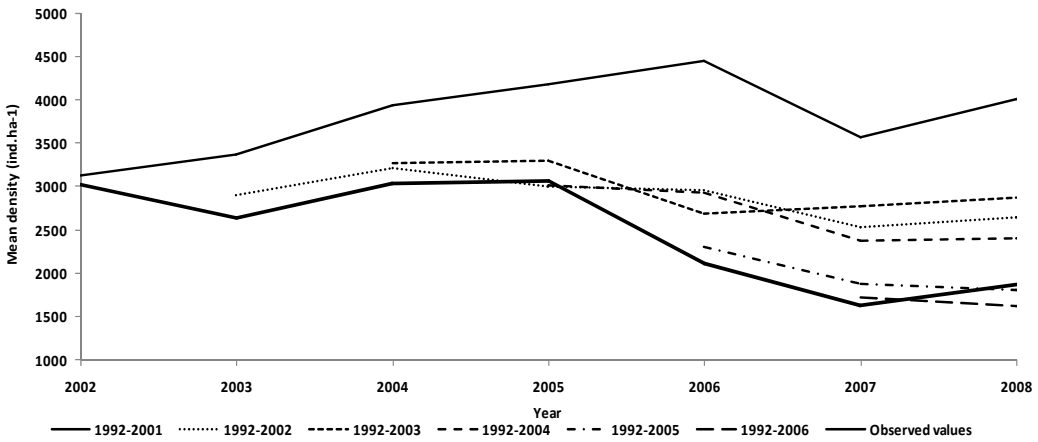

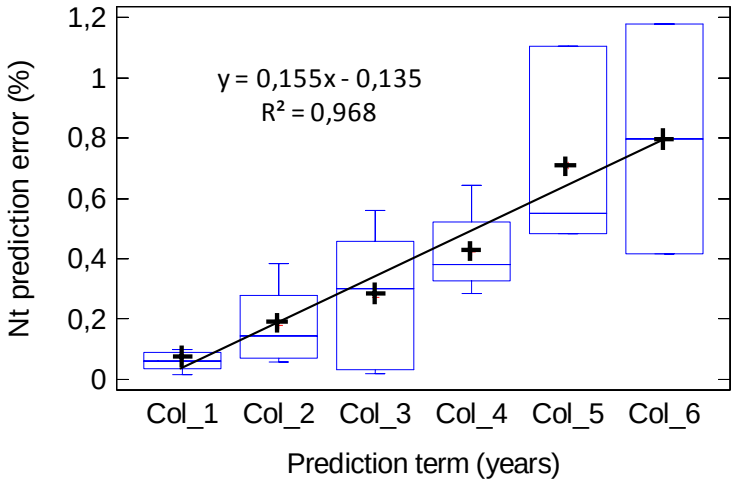

Estimated mean densities N_t obtained from iteration of non-structured (top) and age-structured (bottom) predictive model fitted to different data time series. Standard error of predictions vs. prediction term.

Relevance of recruitment

The whole population is governed by the same drivers as the age class 0+:

$$\lambda_t = k \cdot \frac{1}{N_t} \longrightarrow \lambda^{0+}{}_t = k \cdot \frac{1}{N_t}$$

$$\lambda_t = k.N_{t-2} \longrightarrow \lambda^{0+}{}_t = k.N_{t-2}$$

$$\lambda_t = k.N_t \times NAO_{w,t+1} \longrightarrow \lambda^{0+}{}_t = k.N_t \times NAO_{w,t+1}$$

<u>Conclusion 1:</u> Population size is mainly determined by the size of age class 0+ (recruitment).

Intercohort competition

There is a positive feedback between N_{t-2} (stock of reproducers) and λ^{0+}_t (fry recruitment in year t+1)

$$\lambda^{0+}_t = k \,.\, N_{t-2}$$

Conclusion 2: Stock-recruitment relationship remains in the raising part of the curve.

There is a negative feedback between N_t (mainly fry in year t) and λ^{0+}_t (fry recruitment y year t+1)

$$\lambda^{0+}_t = k \,.\, \frac{1}{N_t}$$

Conclusion 3: Fry recruitment is regulated by competing juveniles (inter-cohort competition).

Discussion

Exogenous limitation: how does NAO_{wt} act?

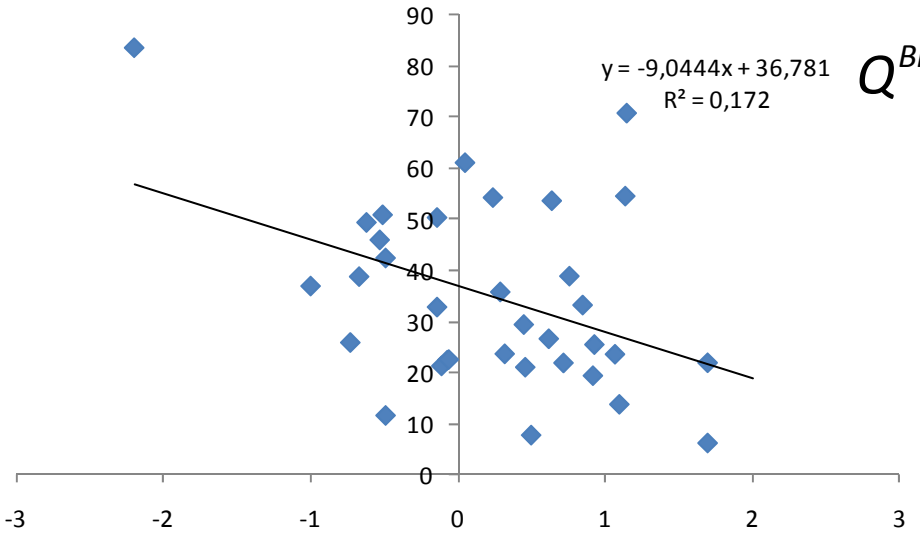

$$Q^{Bidasoa}_{march\_t} = k \cdot \frac{1}{NAO_{w,t}}$$

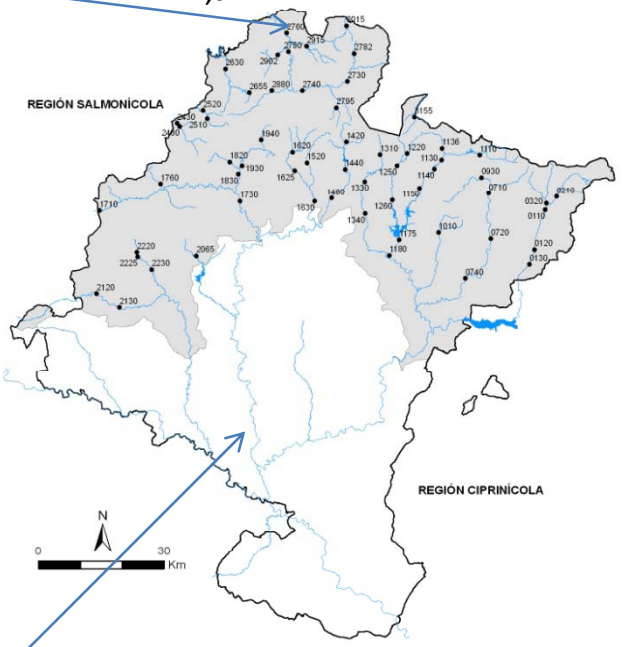

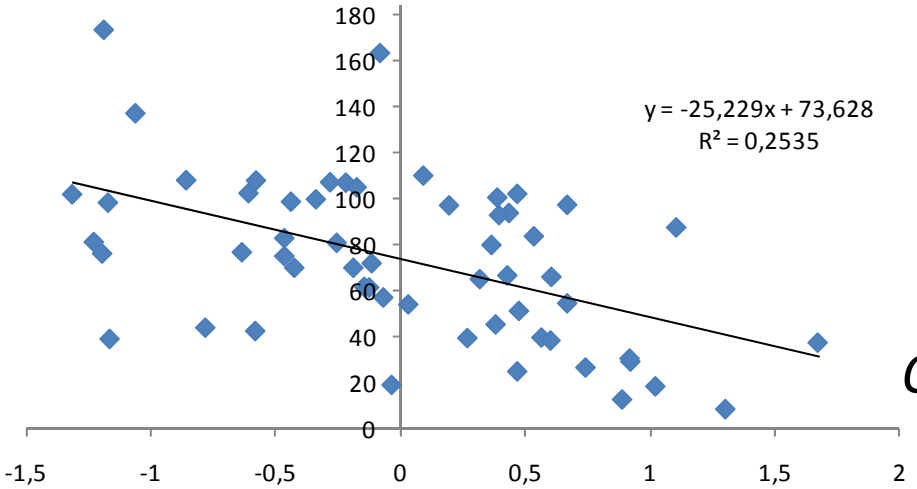

$$Q^{Arga}_{march\_t} = k \cdot \frac{1}{NAO_{w,t}}$$

<u>Conclusion 4:</u> Causal relationship between the biotic answer and the NAO_w acts through hydrological flow regime (namely mean flow in march).

Discussion

How can separated populations have a common response to endogenous factors?

$$r_t = r_0 . \quad (1 - \frac{N_t}{K} \quad)$$

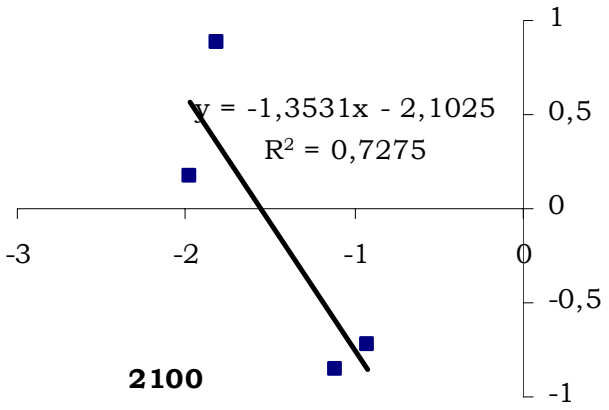

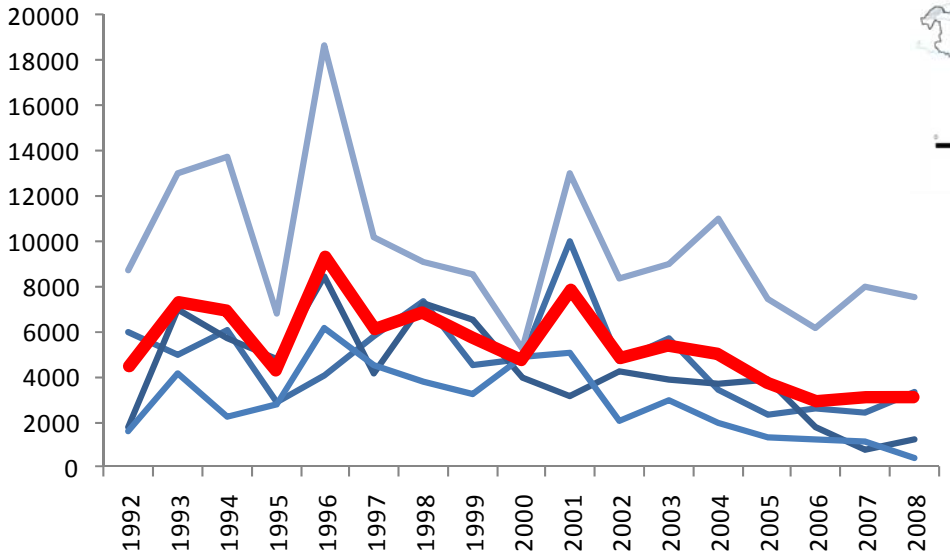

<u>Conclusion 4:</u> Carrying capacity may act as a common starting point for *pgr* of independent populations to fluctuate in synchrony in response to endogenous factors.

Discussion

Which drivers regulate a set of separated populations?

$$\lambda_t = f(NAO_{w,t}, N_t)$$

Population growth rates are synchronized by **Moran effect** (acting through $NAO_{w,t}$) but also by a **simultaneous response of pgr to an endogenous driver.** (N_t).

Large Scale dynamics of Brown trout populations across Navarra' Rivers (North Spain)

THANK YOU FOR YOUR INTEREST

Alonso, C., García de Jalón, D., Álvarez, J. , Gortázar, J.

Advances in the Population Ecology of Stream Salmonids

ecohidráulica

Grupo Investigación HIDROBIOLOGÍA
UNIVERSIDAD POLITÉCNICA DE MADRID

GESTION AMBIENTAL
VIVEROS Y REPOBLACIONES
DE NAVARRA S.A.

Reserva
Reserva

Results

Model plot

Non-structured model

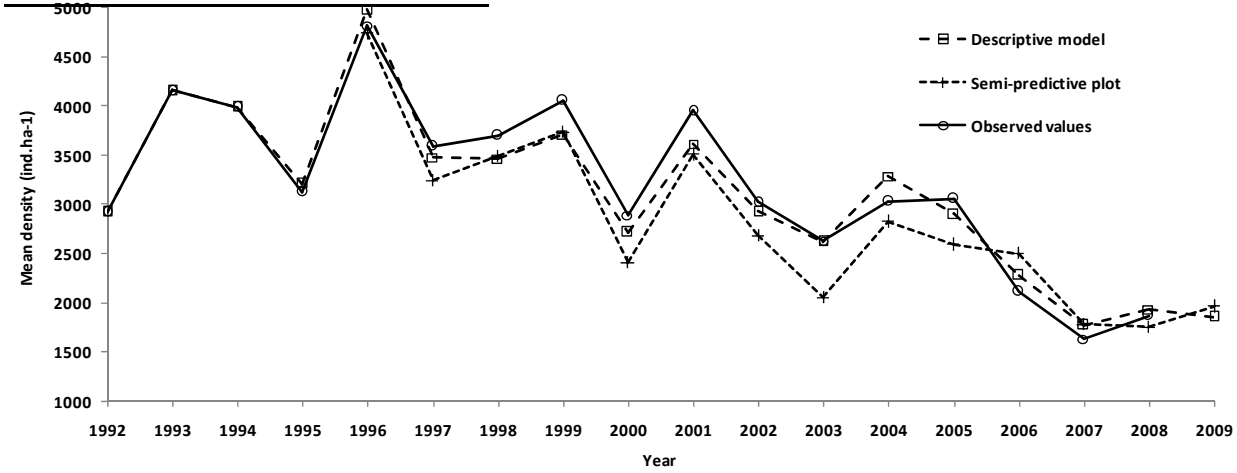

Age-structured model

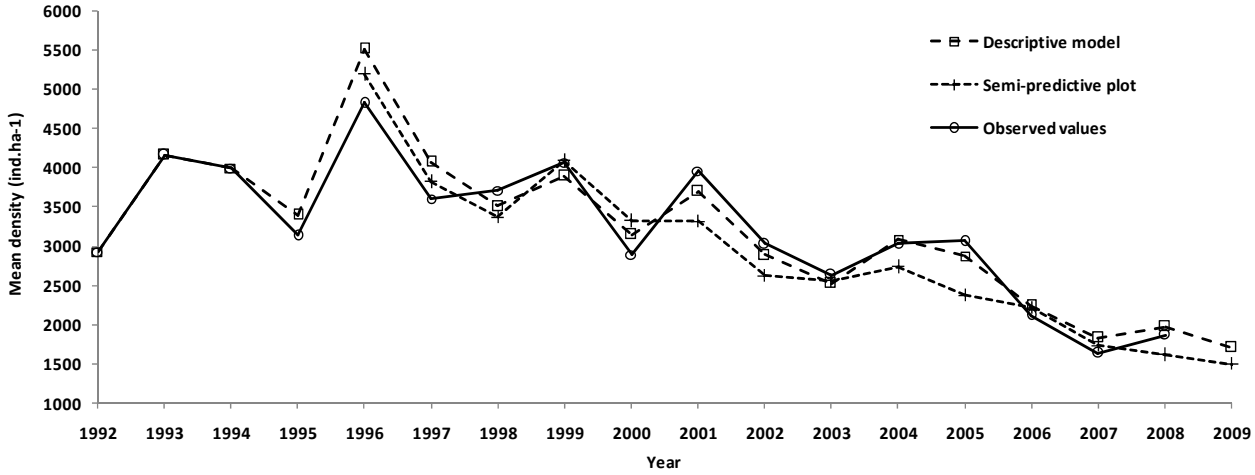

Results of the fitted non-structured (top) and age-structured (bottom) *descriptive and predictive plots* represented against time.

Reserva

Figuras pgr

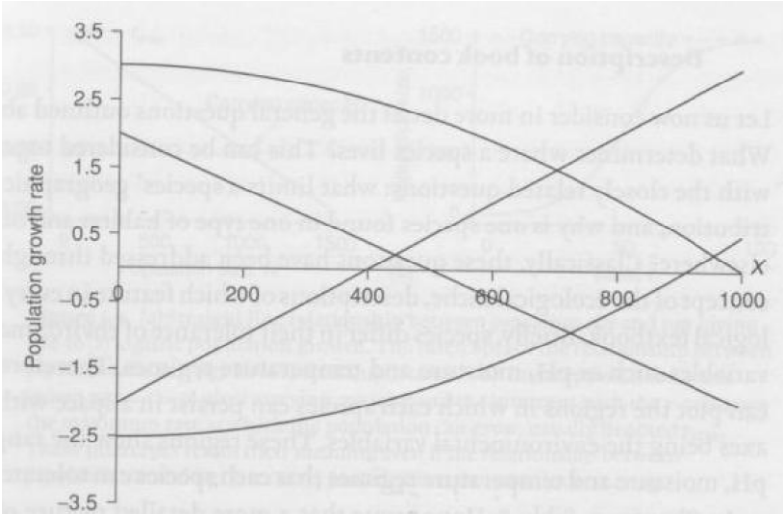

Figure 1.2. Examples of hypothetical linear, nonlinear, positive and negative relationships between demographic, mechanistic and density-dependent determinants (X) of population growth rate.

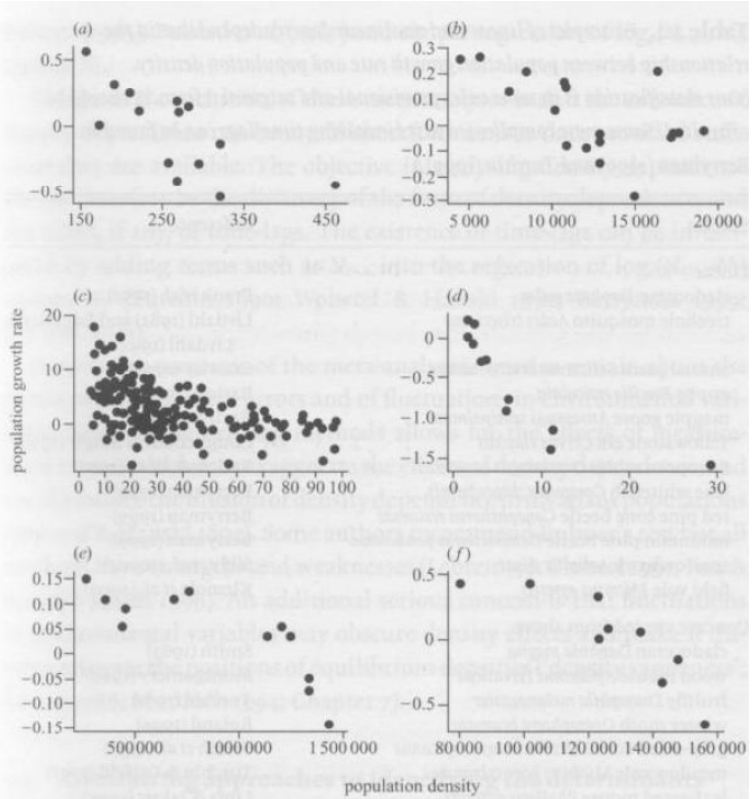

Figure 2.3. Examples of the form of the relationship between population growth rate (r) and population density. Linear relationships in (a) magpie goose and (b) elk; concave viewed from above in (c) meadow vole and (d) arctic ground squirrel; convex viewed from above in (e) wildebeest and (f) sandhill crane. Sources in table 2.1.

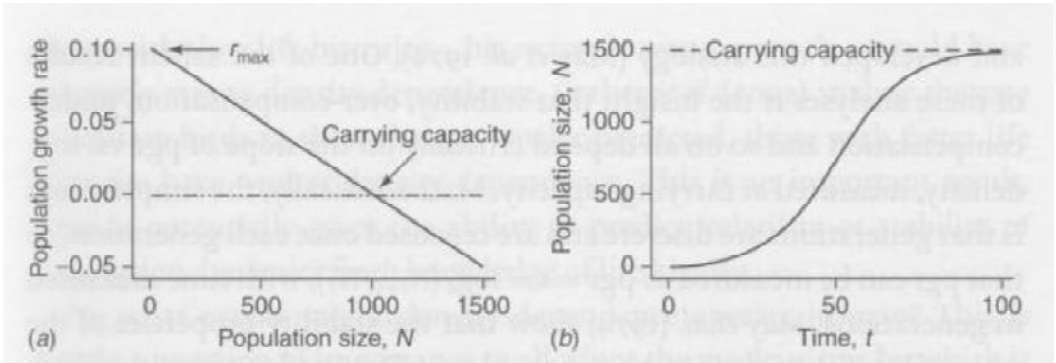

Sibly & Hone (2003)

Planteamiento

Tasa de crecimiento poblacional (*tcp*)

Siendo:

B_t, nº de reclutados en el instante t

D_t, nº de muertos entre t y t+1,

$$N_{t+1} = N_t - D_t + B_t$$

S_t, nº de supervivientes entre t y t+1

$$S_t = N_t - D_t$$

$$N_{t+1} = S_t + B_t$$

λ_t, tasa de crecimiento poblacional *per capita*

$$\lambda_t = \frac{N_{t+1}}{N_t} = \frac{S_t + B_t}{N_t} = \boxed{= s_t + b_t}$$

Planteamiento

Tasa de crecimiento poblacional (*tcp*)

$$N_{t+1} = N_t - D_t + B_t$$

$$B_t - D_t = N_{t+1} - N_t$$

$$N_{t+1} - N_t = \frac{dN}{dt}$$

$$\frac{dN}{dt} = b.N - d.N = (b-d).N = \alpha.N$$

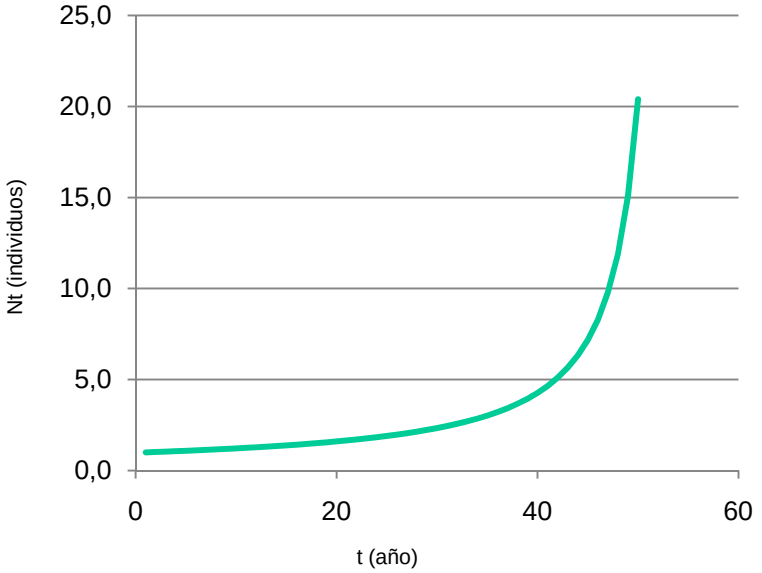

Resultados esperados

Caso de estudio: Navarra-NAO

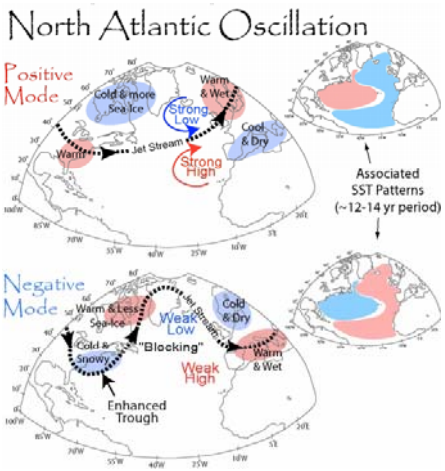

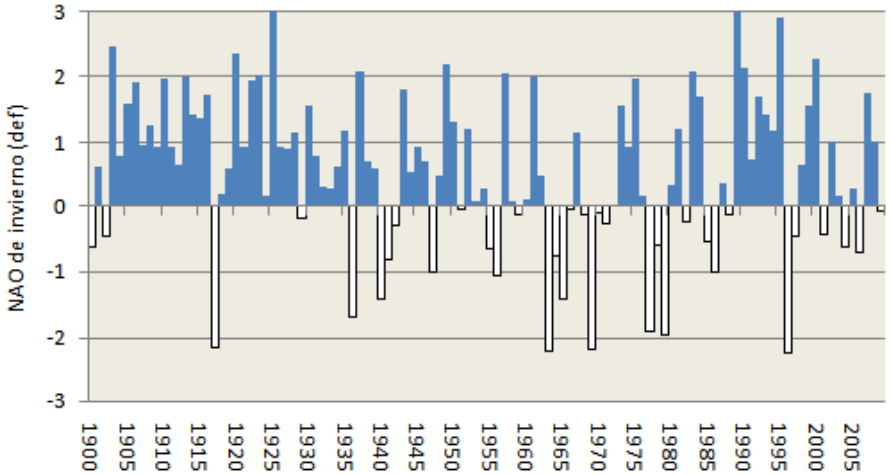

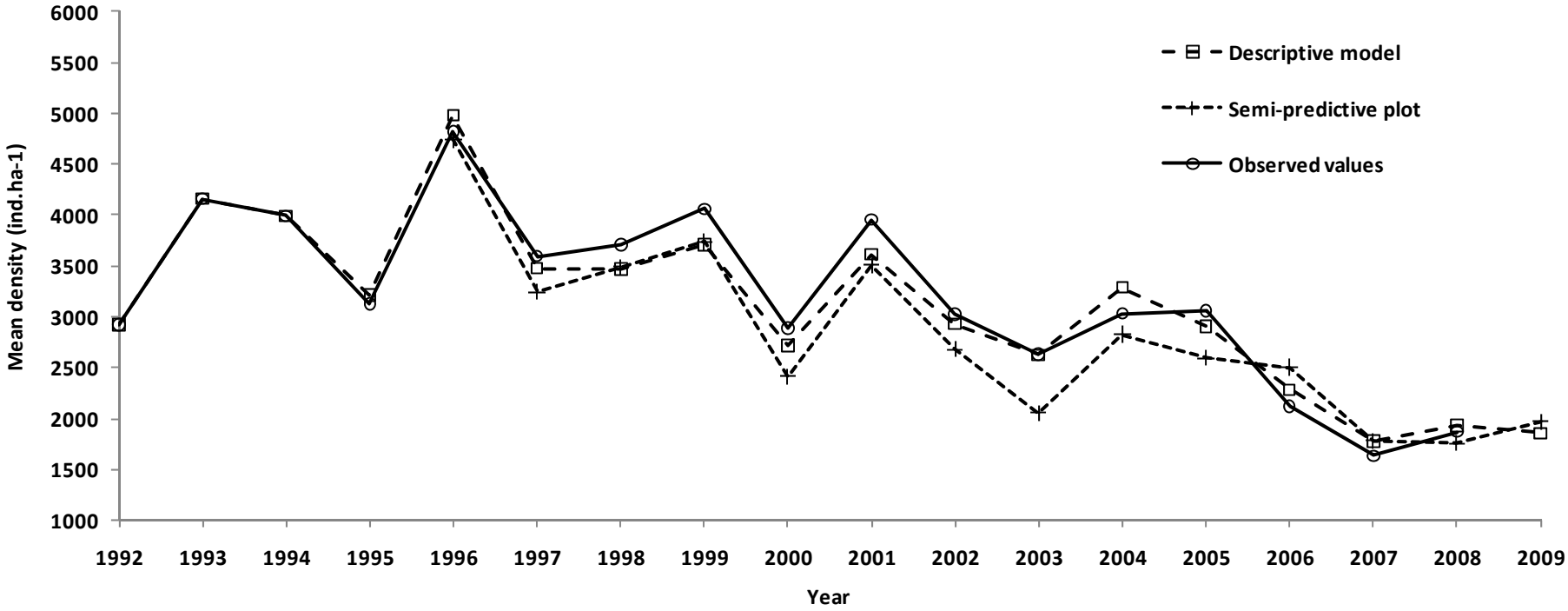

Grupo Investigación HIDROBIOLOGÍA
UNIVERSIDAD POLITÉCNICA DE MADRID

ecohidráulica

Introducción

Área de distribución natural

Studies determining specifically to what extent exogenous factors influence in the temporal dynamics of a given brown trout population

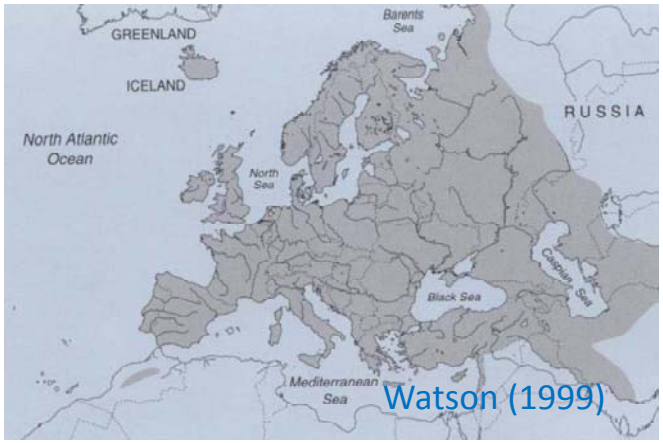

Watson (1999)

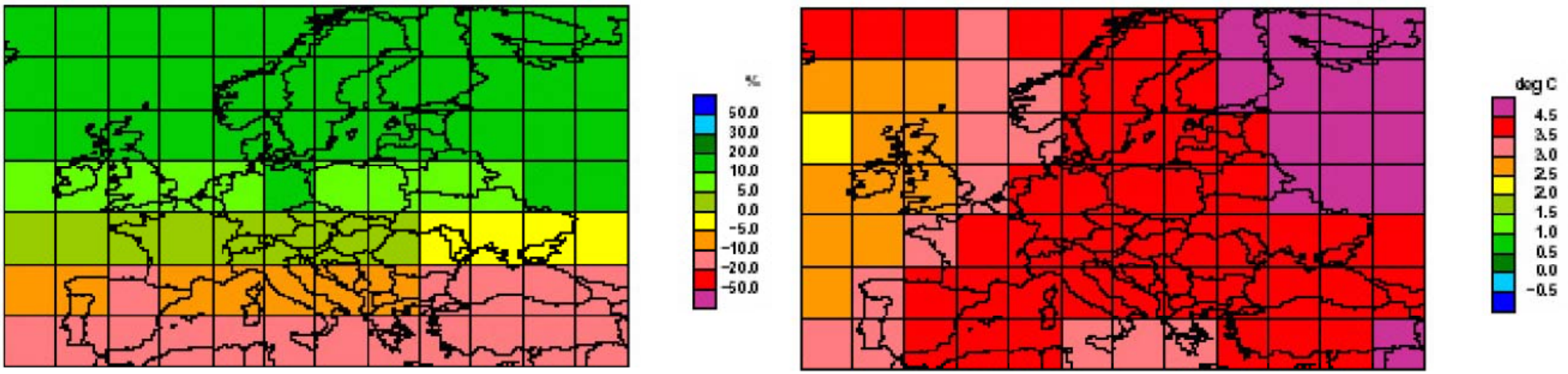

Figura 4.5. Cambio de precipitación (izquierda) y temperatura media (derecha) bajo el escenario de emisión SRES A2 para el período (2086-2115) con respecto al período de referencia (1961-1990) basado en el promedio de 16 AOCGM para el promedio anual (fila 5.ª). Producido con MAGICC-SCENGEN (version 2.4) con la opción de sensibilidad climática media y los parámetros de MAGICC por defecto.

AEMET (2009)

Introducción

Estrategias de vida

Fig. 5. Continuum of life history tactics in the Oir River brown trout (*Salmo trutta*) population: (*a*) males and (*b*) females. In the middle are the different environments in which fish live, migrate, grow, and spawn. A gradient of juvenile growth (first and second years; numbers on inside of graphic) increasing from the centre to the edge is shown below: the thin solid line, thick solid line, and thick broken line represent low, intermediate, and high juvenile growth rate, respectively. An arrow represents 1 year. Numbers along the top indicate age at maturity. A thin dotted line completing the life cycle is present when most of the fish survived after spawning (multispawners).

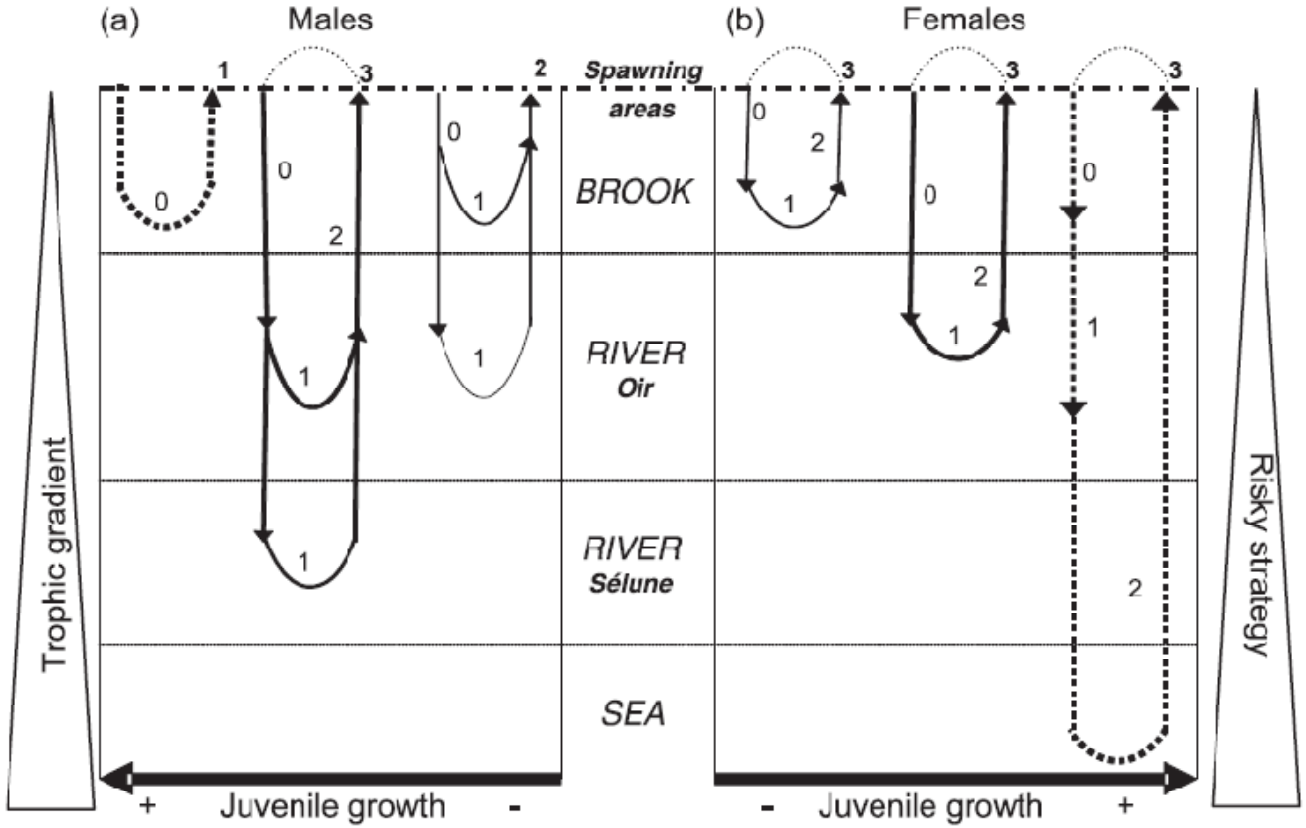

Cucherousset *et al*. (2005)

Grupo Investigación HIDROBIOLOGÍA
UNIVERSIDAD POLITÉCNICA DE MADRID
ecohidráulica

Introducción

Estado del conocimiento (I)

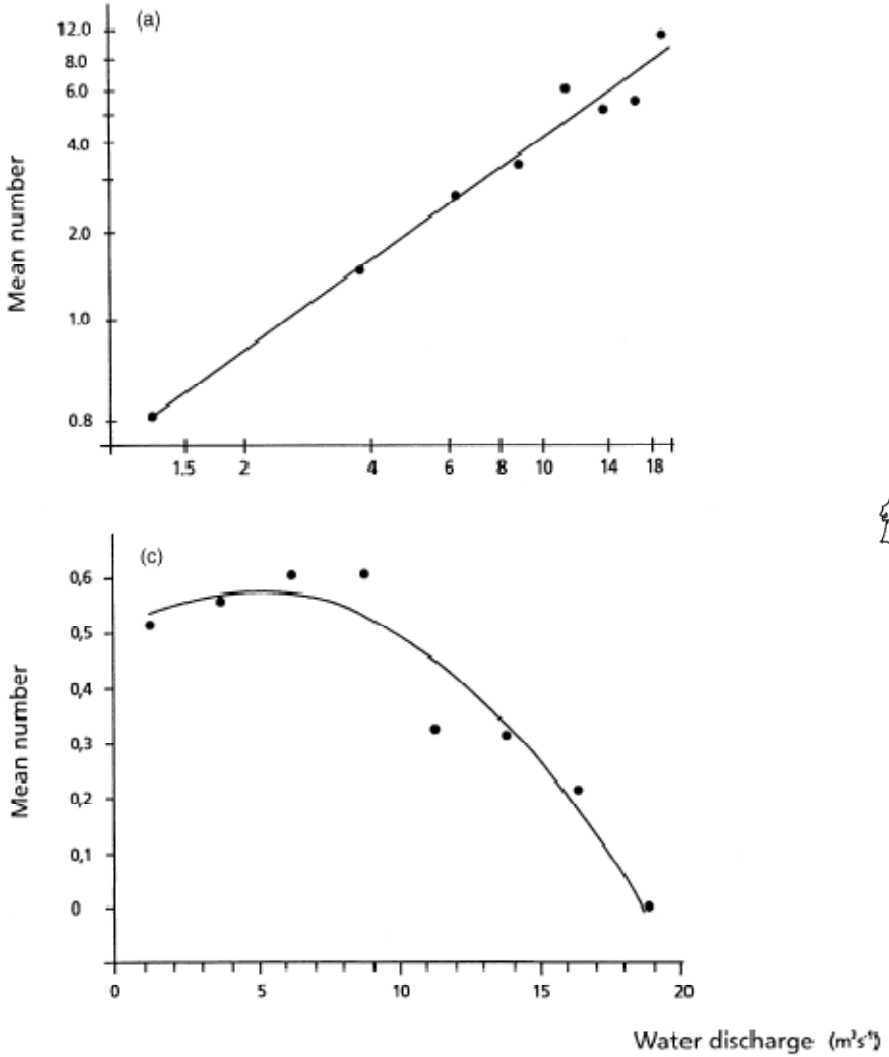

Fig. 6. The relationship between flow and (a) mean number of descending brown trout per day at different median flows (1.25, 3.75, 6.25, 8.75, 11.25, 13.75, 16.25 and 18.75 $m^3 \cdot s^{-1}$) in the River Imsa for fish <30 cm in body length (b) relative river descent (number of trout <30 cm in body length per month/number per year) over mean monthly water flow in between August 1976 and 1999 (c) mean number of ascending brown trout per day at different median flows (as in (a)) between April and December (d) relative ascent in August (number of ascending trout in the month/number in the year) over mean water flow between 1976 and 1999. (Redrawn from Jonsson & Jonsson 2002)

Klemetsen et al. (2003) (de Jonsson & Jonsson 2002)

Grupo Investigación HIDROBIOLOGÍA
UNIVERSIDAD POLITÉCNICA DE MADRID
ecohidráulica

Introducción

Estado del conocimiento (I)

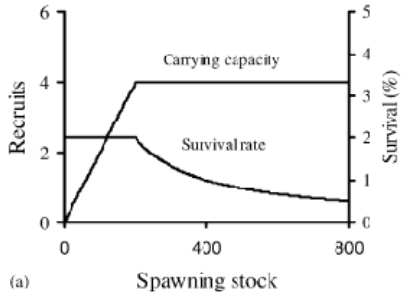

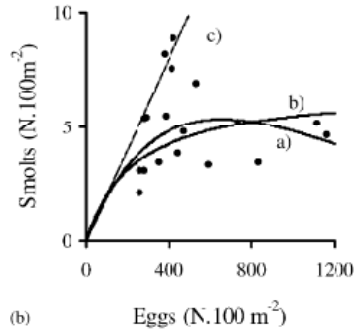

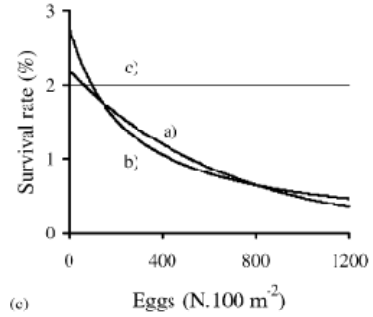

Fig. 1. (a) Diagrammatic representation of recruitment constrained by carrying capacity, showing survival rate (% egg to recruit) changing with spawning stock. (b) Stock-recruit curves for salmon from the River Bush (northern Ireland (adapted from Kennedy and Crozier, 1993), showing (a) dome-shaped (Ricker) and (b) asymptotic (Beverton and Holt) relationships. Line (c) shows directly proportionate survival (egg to smolt) at an arbitrary 2%. (c) Survival rates (%) between egg and smolt stages for the stock–recruitment relationships shown in figure (b).

Milner *et al*. (2003)

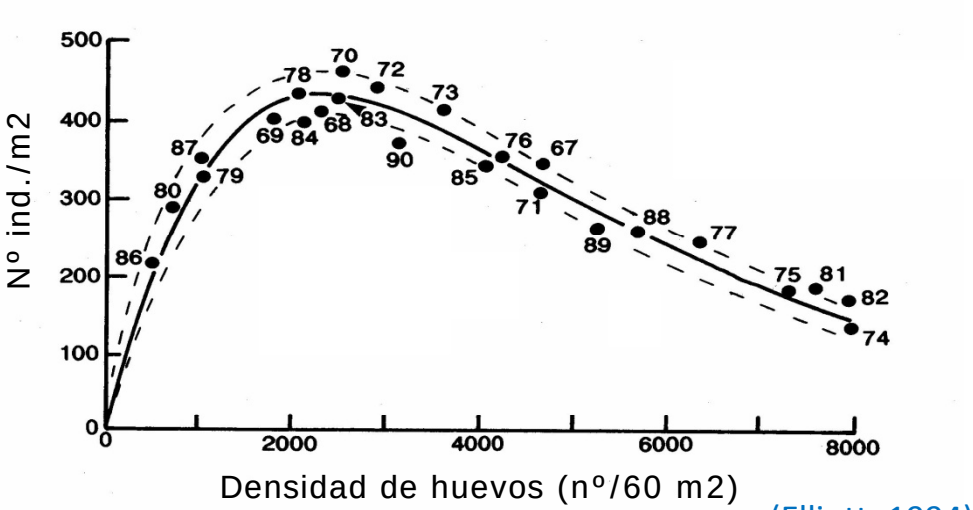

(Elliott, 1994)

Grupo Investigación HIDROBIOLOGÍA
UNIVERSIDAD POLITÉCNICA DE MADRID
ecohidráulica

Introducción

Estado del conocimiento (I)

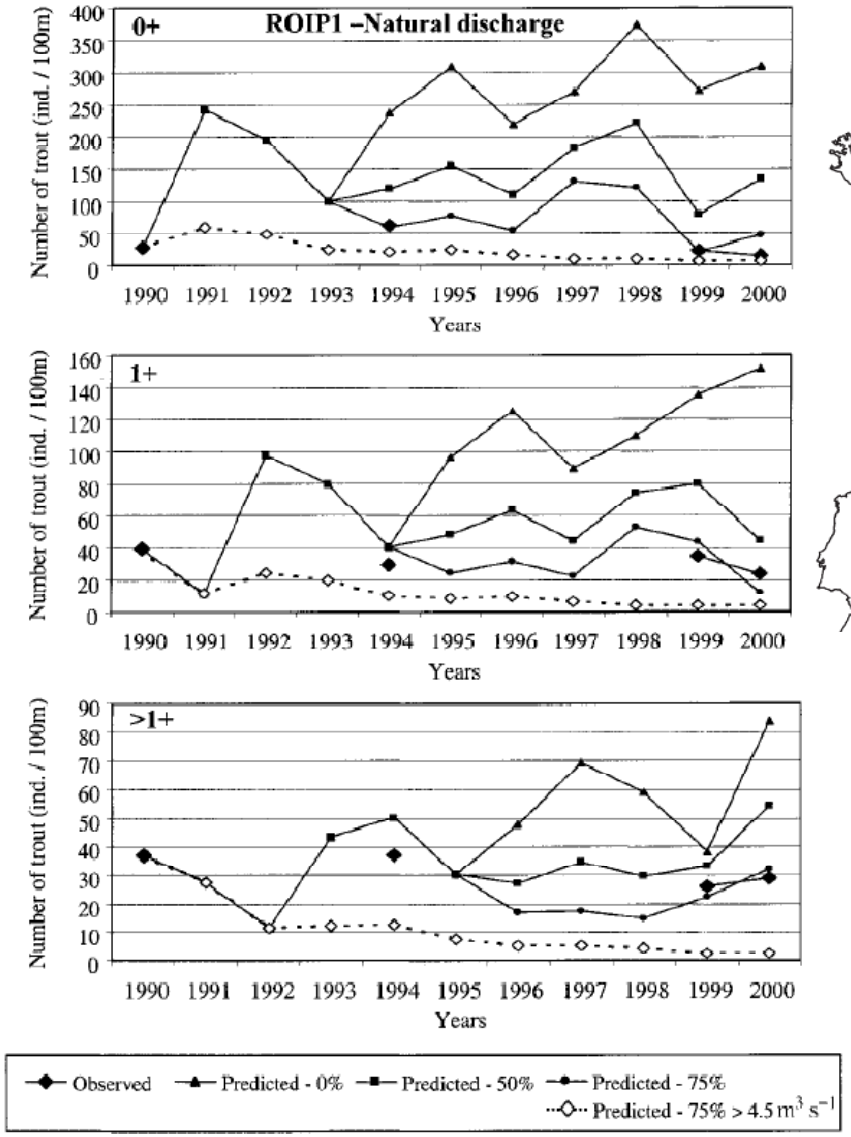

Figure 8. Results of the MODYPOP simulations of trout numbers from 1990 to 2000 in reach 1. The initial state corresponds to that of the populations in 1990. Results are presented for each life stage. Black diamonds represent observed values. Other symbols correspond to predicted values. Predicted values were generated using different supplementary mortality value (0%, triangles; 50%, squares; 75%, circles) for 0+ due to discharge greater than 6.4 $m^3 s^{-1}$, and supplementary mortality (75%) of 0+ due to discharge greater than 4.5 $m^3 s^{-1}$ (white diamonds)

Capra *et al.* (2003)

Grupo Investigación HIDROBIOLOGÍA
UNIVERSIDAD POLITÉCNICA DE MADRID
ecohidráulica

Introducción

Estado del conocimiento (II)

Grupo Investigación HIDROBIOLOGÍA
UNIVERSIDAD POLITÉCNICA DE MADRID

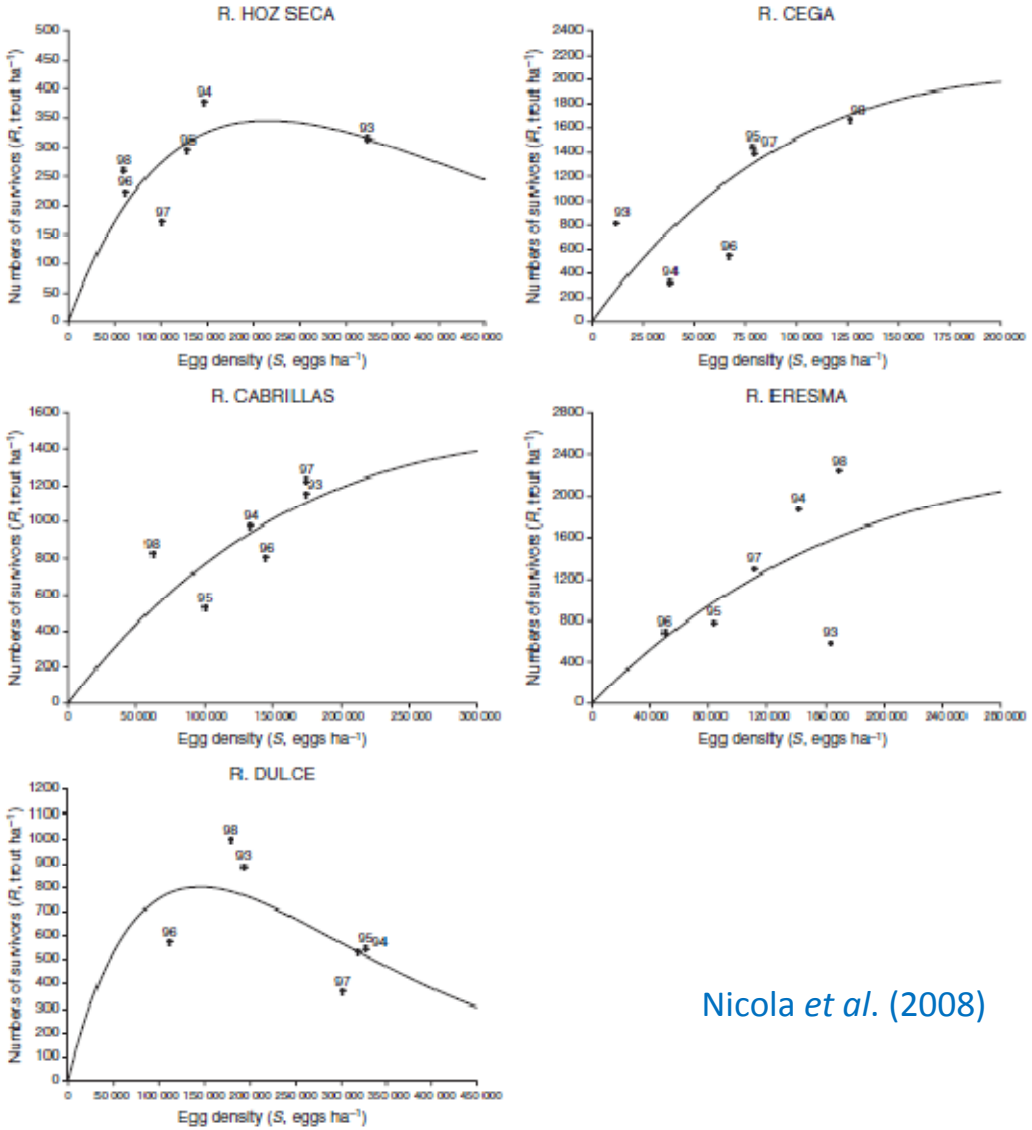

Nicola *et al.* (2008)

Fig. 2 Relationship between the number of recruits (R, trout ha^{-1}) and the initial egg density at the start of each year-class (S, eggs ha^{-1}) in five Spanish rivers from 1992 to 1998. Curves were estimated from Ricker's (1954) equation (see Methods for details). Parameter estimates for the Ricker model are given in Table 3.

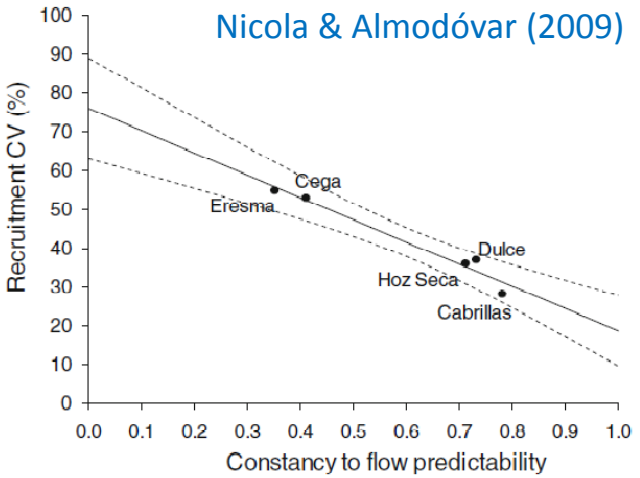

Nicola & Almodóvar (2009)

Fig. 3 Relationship (with 95% confidence intervals) between predictability of daily flow, expressed as the index between constancy and predictability (see "Materials and methods" for more details), and the coefficient of variation for recruitment (0+trout density) during 1992–1998 in five streams from central Spain

Introducción

Estado del conocimiento (II)

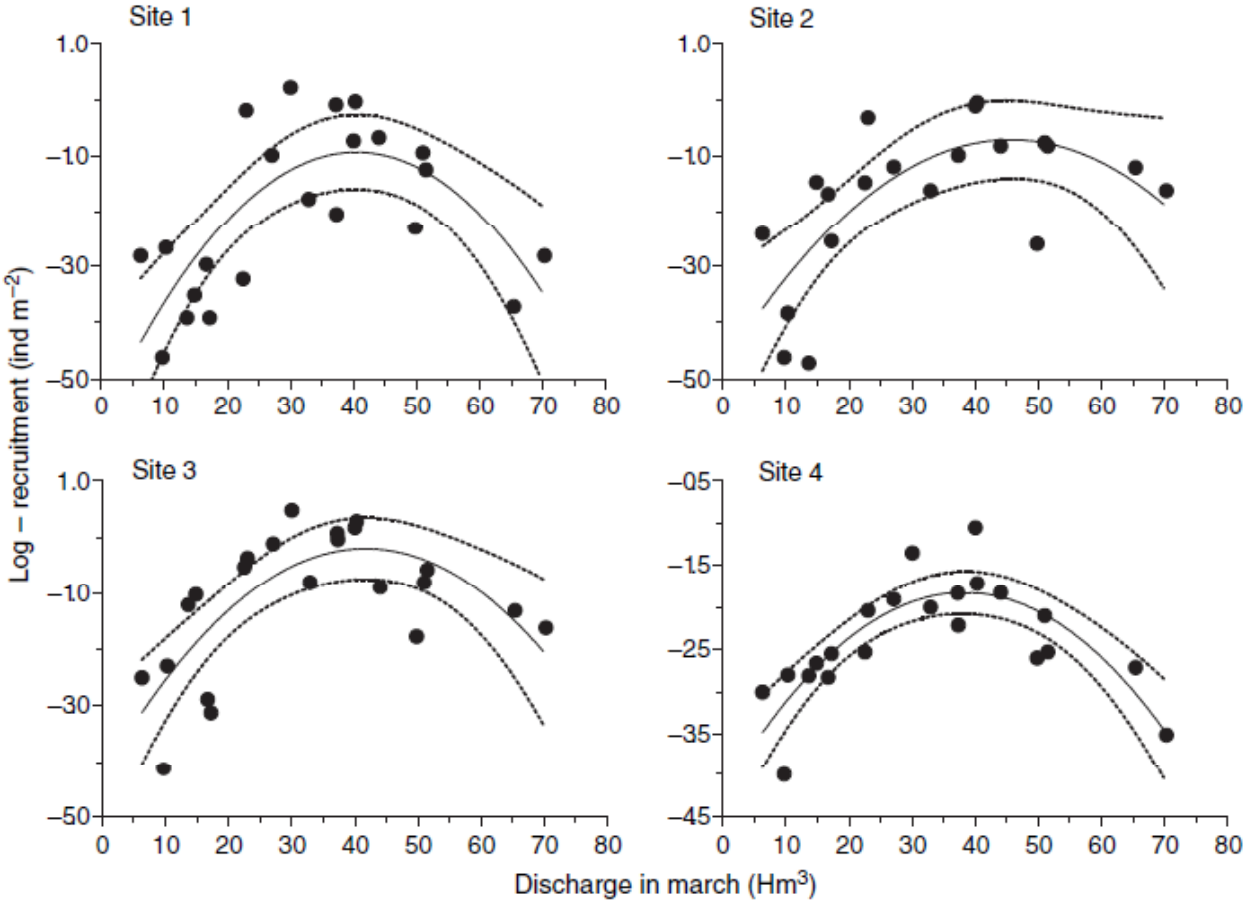

Fig. 4 Increased and decreased patterns depicted by the log-transformed recruitment (R, ind. m^{-2}) against discharge in March (Hm^3) with parabolic functions (±95% CL) fitted to the 22-year data sets recorded at four study sites (sites 1–4) of Rio Chaballos (Rio Esva drainage, northwestern Spain).

Lobón-Cerviá (2009)

Introducción

Estado del conocimiento (II)

Grupo Investigación HIDROBIOLOGÍA
UNIVERSIDAD POLITÉCNICA DE MADRID

ecohidráulica

Fig. 3 Regression analyses and proportion of variability (R^2) of population variables explained by flow metrics by means of linear models

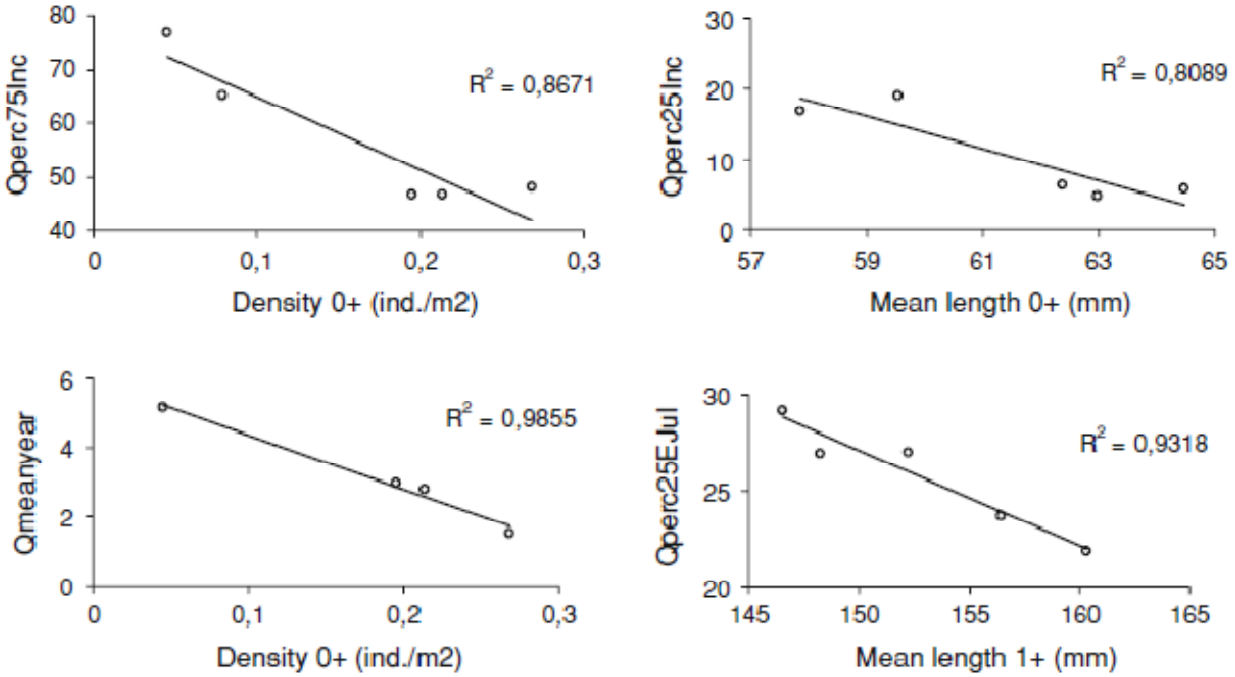

Alonso *et al*. (2008)

Introducción

Estado del conocimiento (II)

Grupo Investigación HIDROBIOLOGÍA
UNIVERSIDAD POLITÉCNICA DE MADRID

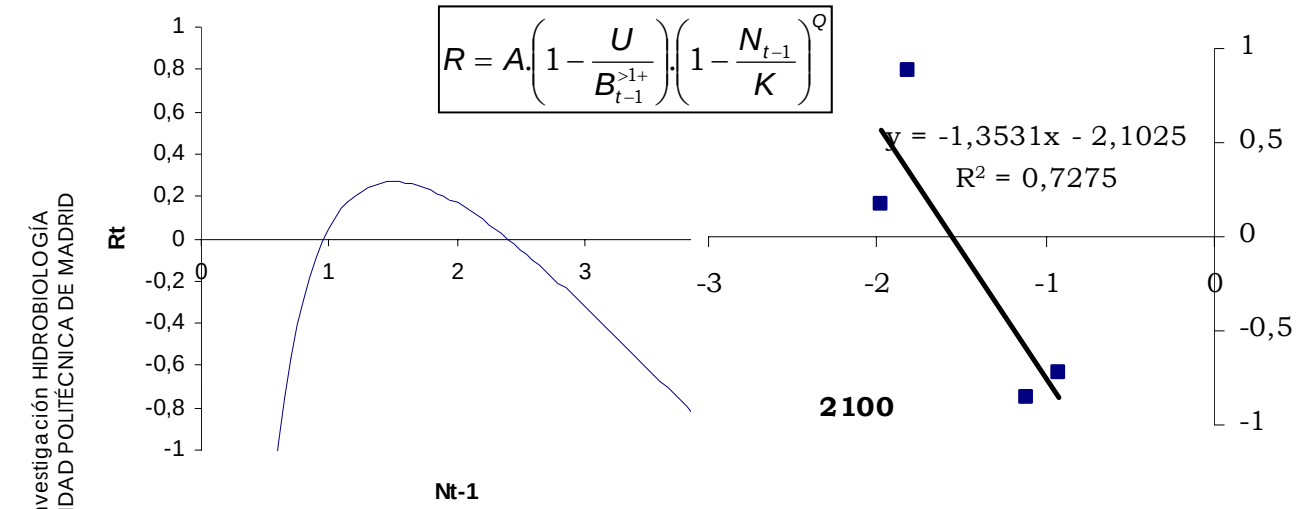

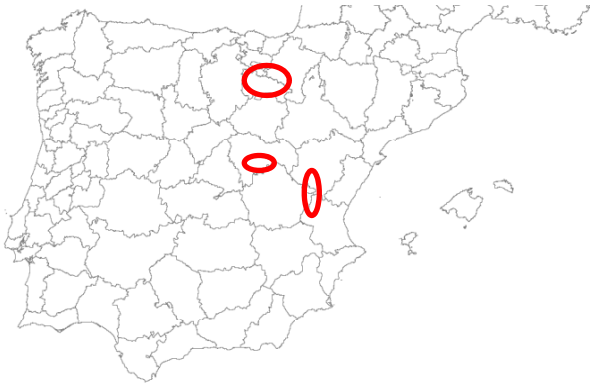

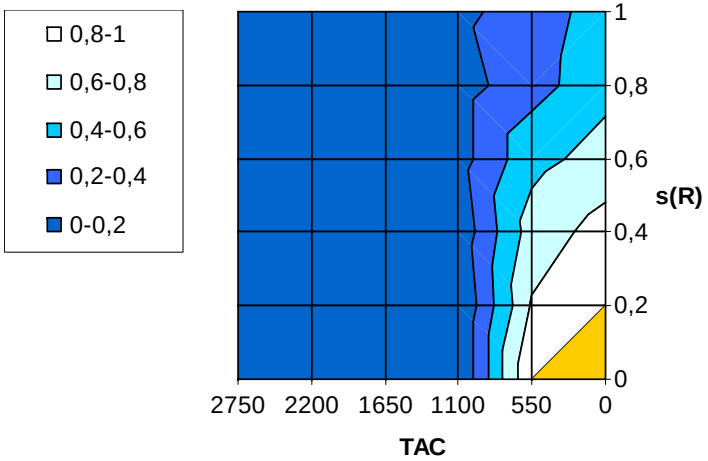

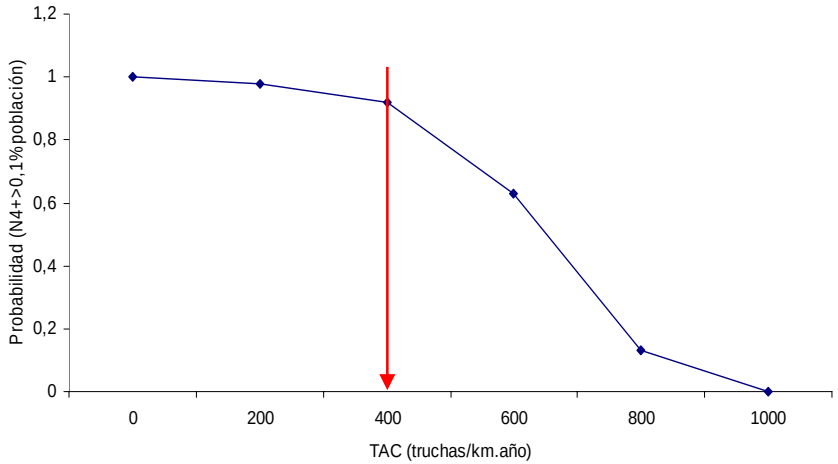

Alonso *et al*. (2007); Gortázar *et al*. (2009, 2010)

Discussion

Endogenous regulation: relevance of recruitment

$$\lambda^{1+}{}_t = k \quad NAO_{wt}$$

when NAO_{wt} is high, then $\lambda^{1+}{}_t$ is high, and then $\lambda^{1}{}_t$ is low (1)

$$\lambda_t = k \cdot \frac{1}{NAO_{wt}}$$

when NAOwt is high, then λt is low (2)

Furthermore: $\lambda_t = k \cdot \frac{1}{N_t}$ and $\lambda_t = k \cdot N_{t-2}$

In the same way: $\lambda^{0+}{}_t = k \quad \frac{1}{N_t}$ and $\lambda^{0+}{}_t = k \quad N_{t\ 2}$

<u>Conclusion 1:</u> Population size is mainly determined by age class 0+ size (recruitment).

Results

Observed vs. modeled

Non-structured model

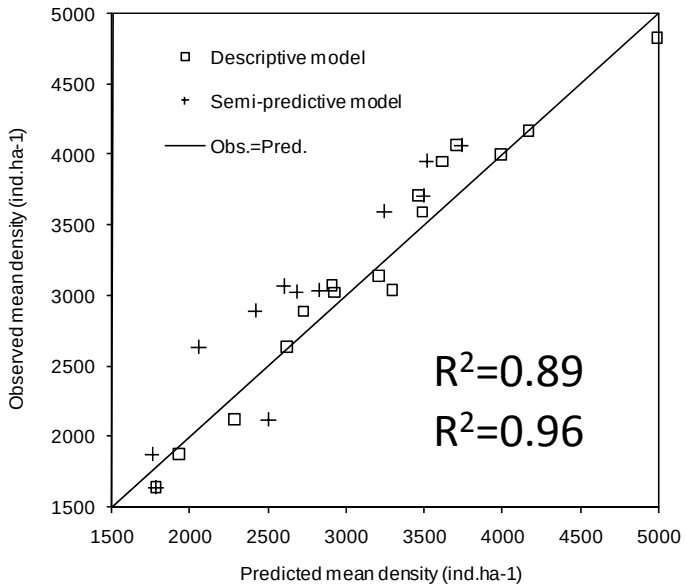

Age-structured model

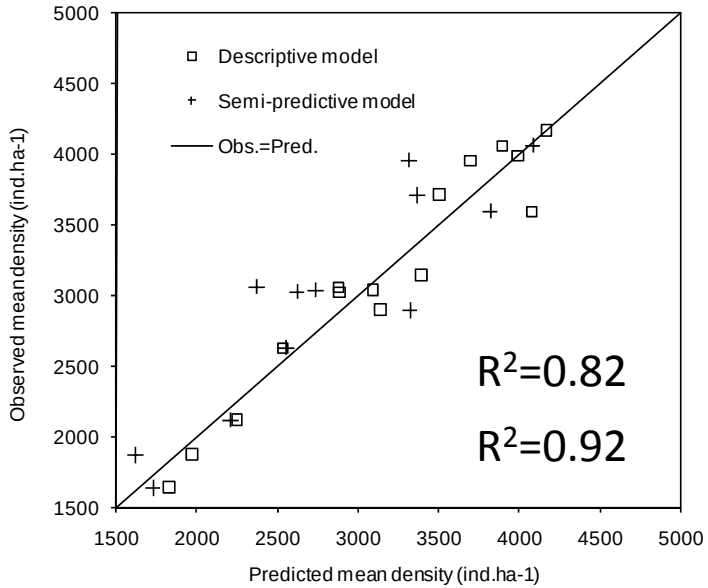

Results of the fitted non-structured (left) and age-structured (right) *descriptive plot* and *predictive plot*, observed versus predicted graph.

Results

Prediction errors

Non-structured model

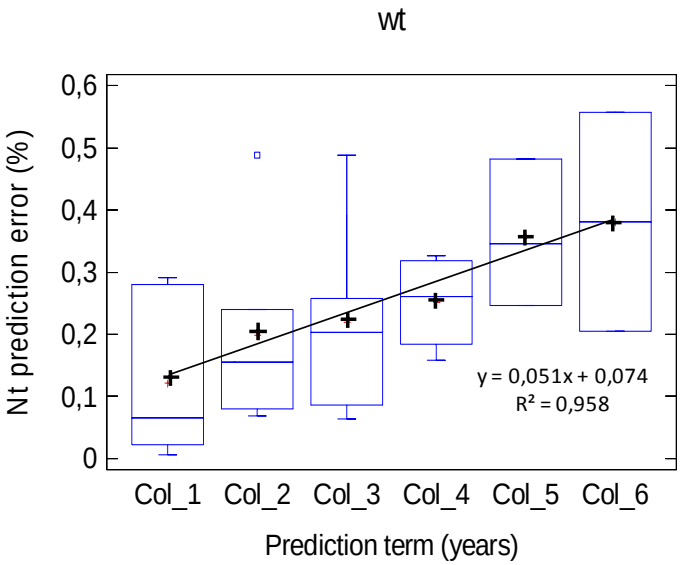

Age-structured model

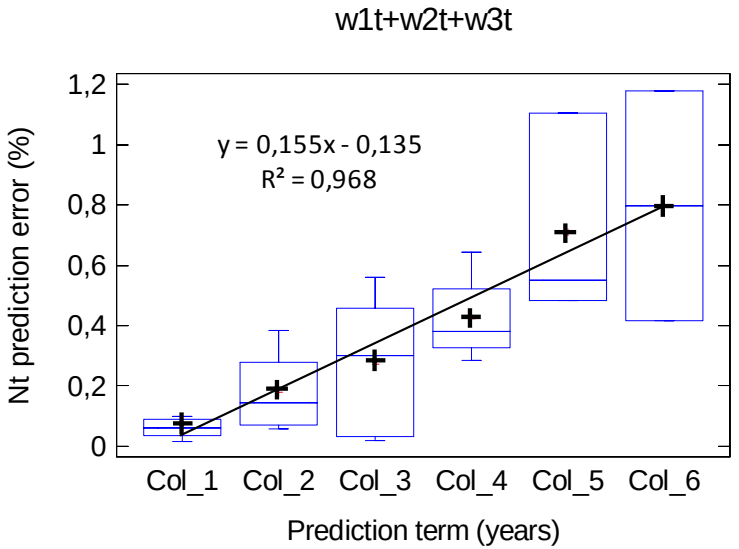

Standard errors of mean density Nt predicted for the following years after the end of the data time series subset used to fit each predictive model plotted against the prediction term in years.